J. Electrochem. Sci. Eng. **8(1)** (2018) 3-37; DOI: http://dx.doi.org/10.5599/jese.448

Open Access : : ISSN 1847-9286

www.jESE-online.org

Review article

Conducting polymers: past, present, future

György Inzelt

Department of Physical Chemistry, Institute of Chemistry, Eötvös Loránd University, Pázmány Péter sétány 1/A, 1117 Budapest, Hungary

E-mail: inzeltgy@chem.elte.hu

Received: September 29, 2017; Revised: October 30, 2017; Accepted: November 2, 2017

Abstract

In my plenary lecture delivered at the 6th Regional Symposium on Electrochemistry of South-East Europe (RSE-SEE) that was held between June 11 and 15, 2017, in Balatonkenese, Hungary I surveyed the developments in the field of conducting polymers based on my 40 years of experience in this area. It is intended to give an overview including thermodynamical considerations, redox transformations and transport processes, methods of investigation, redox polymers, electropolymerization, characterization, and applications with abundant examples from my research results.

Keywords

Synthesis; Redox behaviour; Composites; Sensors; Biosensors; Supercapacitors; Electrocatalysis

Introduction

The preparation, characterization and application of electrochemically active, electronically conducting polymeric systems are still at the foreground of research activity in electrochemistry [1-3]. There are at least two major reasons for this intense interest. First is the intellectual curiosity [1-4] of scientists, which focuses on understanding the behavior of these systems, in particular on the mechanism of charge transfer and on charge transport processes that occur during redox reactions of conducting polymeric materials [2, 4-6]. Second is the wide range of promising applications of these compounds in the fields of energy storage, electrocatalysis, organic electrochemistry, bioelectrochemistry, photoelectrochemistry, electroanalysis, sensors, electrochromic displays, microsystem technologies, electronic devices, microwave screening and corrosion protection [2]. After 40 years of research in the field, the fundamental nature of charge propagation is now in general understood; *i.e.*, the transport of electrons can be assumed to occur via an electron exchange reaction (electron hopping) between neighboring redox sites in redox polymers, and by the movement of delocalized electrons through conjugated systems in the case of so-called intrinsically conducting polymers (*e.g.*, polyaniline, polypyrrole). (In fact, several conduction

mechanisms, such as variable-range electron hopping and fluctuation-induced tunneling, have been considered.) In almost every case, the charge is also carried by the movement of electroinactive ions during electrolysis; in other words, these materials constitute mixed conductors [2,5,6]. Owing to the diversity and complexity of these systems — just consider the chemical changes (dimerization, cross-linking, ion-pair formation, *etc.*) and polymeric properties (chain and segmental motions, changes in the morphology, slow relaxation) associated with them, the discovery of each new system brings new problems to solve, and much more research is still needed to achieve a detailed understanding of all of the processes related to the dynamic and static properties of various interacting molecules confined in a polymer network.

Although the conductivity of these polymers is an interesting and a utilizable property in itself, their most important feature is the *variability of their conductivity*, *i.e.*, the ease with which the materials can be reversibly switched between their insulating and conducting forms (Figure 1). (The conductivity of copper is still better but not variable!)

An evidence of the existence of the mobile electrons in the system is the practically uniform absorbance at high wavelengths in half-oxidized state (emeraldine form of polyaniline). It is characteristic to the metals (metallic conduction) since the excitation of the mobile electrons needs small and practically the same energy. At lower wavelenghts the variation of the spectra indicates the color change related to the leucoemeraldine – emeraldine – pernigraniline transitions (Figure 2).

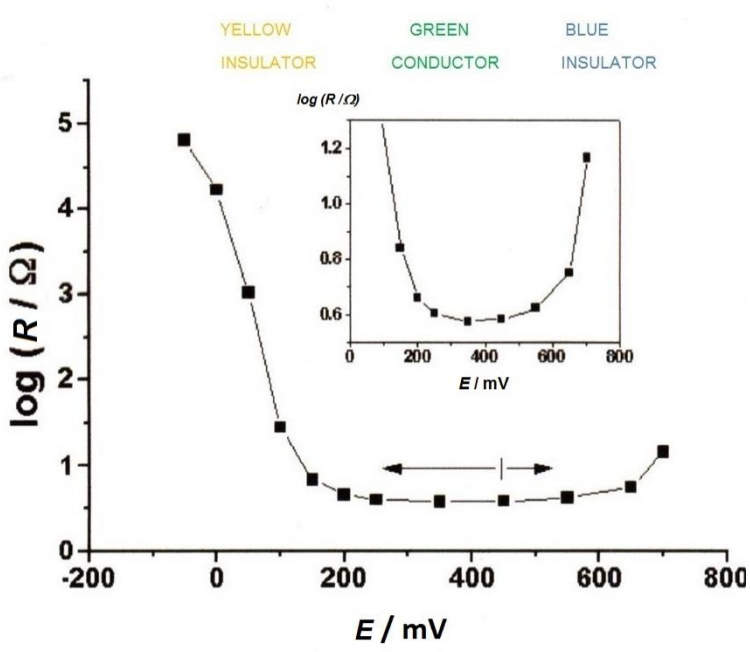

Figure 1. *Variation of the resistance of polyaniline as a function of potential (charging state) in contact with 1 mol dm^{-3} H_2SO_4 (compiled from the results of [7])*

We can utilize the variation of the conductivity in electronic devices including thin film transistors and insulated gate field effect transistors or in gas sensors; the color change in electrochromic display devices or in smart windows, the electroluminescence in light emitting devices, the swelling-deswelling accompanying the charging-discharging processes in artificial muscles, the charge storage capacity in energy technologies (batteries, supercapacitors). There are properties, which are useful in a certain application, *e.g.*, volume change, however, those may cause problem in other utilization. In fact, during the redox transformations generally we create a polyelectrolyte from an uncharged polymer, which alter many physical and chemical properties. For instance, the charged,

salt-form is insoluble, while the neutral form is soluble in certain organic solvents. The overcharging (overoxidation) may lead to the hydrolytic degradation of the polymer. In some cases the mechanical properties including adhesion is of importance, e. g., in corrosion protection or in membranes where gas evolution occurs, which are less crucial in batteries. In the early period several attempts were made to vary the morphology and the swelling properties by using different counterions. The derivatization of the monomers frequently lead to more flexible polymers.

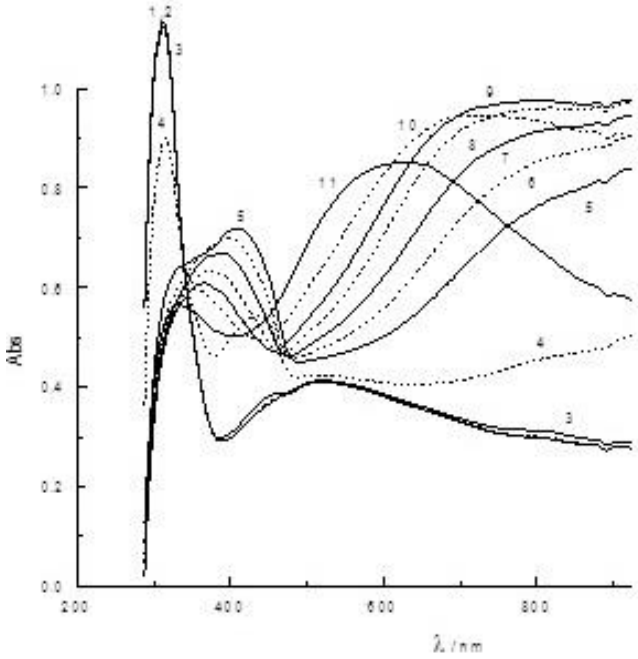

Figure 2. *UV–VIS–NIR spectra of PANI obtained in situ at different potentials: (1) −0.35, (2) −0.25, (3) −0.15, (4) −0.05, (5) 0.05, (6) 0.15, (7) 0.25, (8) 0.35, (9) 0.45, (10) 0.55, and (11) 0.65 V. Solution: 1 mol dm^{-3} H_2SO_4 [8]*

In the last decade the researchers have started to apply novel approaches. The new trend is the fabrication of composites including nanocomposites of polymers and other materials such as carbon nanotubes, graphene or inorganic compounds having special structure and properties. In sensors and biosensors of different kinds (conductometric, impedimetric, potentiometric, amperometric and voltammetric) conducting polymers are used as active, sensing or catalytic layers, however, in the the majority of application those serve as matrices entrapping enzymes or other biologically active compounds. The biocompatibility of several conducting polymers provides opportunity for the application in medicine as artificial muscles and limbs, as well as artificial nerves. The biomimetic (bionic) applications certainly will continue in the future. (References [1-6] contain hundreds of cited papers which were considered by the author as the most important ones. Therefore, most of the citations in this review are the author's works in connection with the results presented. It is worth to mention that the total number of papers on counducting polymers until 2017 according to the scientific database is ca. 300 000 [1].)

Historical background

Somewhat surprisingly, a new class of polymers possessing high electronic conductivity (electronically conducting polymers) in the partially oxidized state was discovered. Alan J. Heeger, Alan G. MacDiarmid and Hideki Shirakawa played a major role in this breakthrough, and they received the Nobel Prize in Chemistry in 2000 "for the discovery and development of electronically conductive polymers" [9-14]. The preparation of polyacetylene and the discovery of the large

increase in its conductivity after "doping" actually launched this new field of research. However, as Thomas Mann wrote: "Very deep is the well of the past". Our case is also curious because the most important representatives of these materials, polyaniline and polypyrrole, were already being prepared by chemical or electrochemical oxidation in the nineteenth century. Of course, for a long time they were not called polymers, since the existence of macromolecules was not accepted until the 1920s. Therefore, it is somewhat interesting to review the story of polyaniline here, because it provides an insight into the nature of the development of science. One may recall that aniline was prepared from the coal tar residues of the gas industry in the first half of the nineteenth century, and later played a fundamental role in the development of organic chemistry and the chemical industry. First, aniline dyes replaced dyes from natural sources. Then coal tar dyes found use in medicine (to stain tissues), and the selective toxicity of these compounds was also discovered. This initiated the chemical production of medicines, and the establishment of the pharmaceutical industry. In 1862 Dr. Henry Letheby, who was a physician and a member of the Board of Health in London, was interested in aniline because it was poisoning workers. Letheby observed that a bluish-green precipitate was formed at the anode during electrolysis, which became colorless when it was reduced and regained its blue color when it was oxidized again [15]. In 1840 Fritzsche observed the appearance of a blue color during the oxidation of aniline in acidic media [16]. In 1950 Khomutov and Gorbachev discovered the autocatalytic nature of the electrooxidation of aniline [17]. In 1962 Mohilner, Adams and Argersinger reinvestigated the mechanism of the electrooxidation of aniline in aqueous sulfuric acid solution at a platinum electrode. They proposed a free radical mechanism, and wrote that "the final product of this electrode reaction is primarily the octamer emeraldine, or a very similar compound" [18].

The first real breakthrough came in 1967, when Buvet delivered a lecture at the 18th Meeting of CITCE (later ISE), and this presentation appeared a year later in Electrochimica Acta [19]. Here we cite the first sentence of this paper, which speaks for itself: "Polyanilines are particularly representative materials in the field of organic protolytic polyconjugated macromolecular semiconductors, because of their constitution and chemical properties". They also established that polyanilines "also have redox properties," and that "the conductivity appears to be electronic". It was also shown that "polyanilines are also ion-exchangers". Finally, they proposed that "polyanilines... can be utilized for making accumulators with organic compounds". While Josefowicz et al. used chemically prepared PANI pellets as an electrode and for conductivity measurements, investigations of the mechanism of electrochemical oxidation also continued, and the name polyaniline became generally accepted. The paper of Diaz and Logan that appeared in 1980 [20] initiated research into polymer film electrodes based on polyaniline, which continues even today.

Definition and classification

Electrochemically active polymers can be classified into several categories based on the mode of charge propagation (note that insulating polymers are not considered here except for those with variable conductivity). The mode of charge propagation is linked to the chemical structure of the polymer. The two main categories are electron-conducting polymers and proton (ion)-conducting polymers. We will focus on electron-conducting polymers here.

We can also distinguish between two main classes of electron-conducting polymers based on the mode of electron transport: redox polymers and electronically (intrinsically) conducting polymers (ECPs or ICPs).

Redox polymers contain electrostatically and spatially localized redox sites which can be oxidized or reduced, and the electrons are transported by an electron exchange reaction (electron hopping) between neighboring redox sites if the segmental motions enable this. Redox polymers can be divided into several subclasses: i) polymers that contain covalently attached redox sites, either built into the chain, or as pendant groups; the redox centers are mostly organic or organometallic molecules; ii) ion-exchange polymeric systems (polyelectrolytes) where the redox active ions (mostly complex compounds) are held by electrostatic binding.

A simple distinction between the intrinsically conducting and redox polymers is that in dry state the ICPs are conducting while redox polymers are not. In the case of redox polymers water (or other solvent) acts as a plasticizer, and makes the chain and segmental motions possible which is inevitable to ensure the electron hopping between the localized redox groups.

Conducting polymers are mostly used as polymer film electrodes by electrochemists. A polymer film electrode can be defined as an electrochemical system in which at least three phases are contacted successively in such a way that between a first-order conductor (usually a metal) and a second-order conductor (usually an electrolyte solution) is an electrochemically active polymer layer which is usually a mixed conductor. The polymer layer is more or less stably attached to the metal, mainly by adsorption (adhesion).

Methods of investigation

Conducting polymers have been studied using the whole arsenal of methods available to chemists and physicists [2]. Electrochemical techniques, mostly transient methods such as cyclic voltammetry (CV), chronoamperometry (CA) and chronocoulometry (CC), are the primary tools used to follow the formation and deposition of polymers, as well as the kinetics of their charge transport processes. Electrochemical impedance spectroscopy (EIS) has become the most powerful technique used to obtain kinetic parameters such as the rate of charge transfer, diffusion coefficients (and their dependence on potential), the double layer capacity, the pseudocapacitance of the polymer film, and the resistance of the film [21].

The application of combinations of electrochemical methods with non-electrochemical techniques, especially spectroelectrochemistry (UV-VIS, FTIR, ESR), the electrochemical quartz crystal nanobalance (EQCN), radiotracer methods, probe beam deflection (PBD), various microscopies (STM, AFM, SECM), ellipsometry, and in situ conductivity measurements, has enhanced our understanding of the nature of charge transport and charge transfer processes, structure–property relationships, and the mechanisms of chemical transformations that occur during charging/discharging processes. In several cases to elucidate more complicated reaction mechanism it is necessary to apply the combination of more than one technique, *e.g.*, transient electrochemical technique with UV-VIS spectroelectrochemistry and ESR, or with spectroelectrochemistry and EQCN.

It is not necessary to deal with these techniques in detail here, since there are several books, monographs and papers on the subject [2, 21-24].

Preparation of conducting polymers

Both redox and electronically conducting polymers can be prepared using chemical and/or electrochemical methods of polymerization, although most redox polymers have been synthesized by chemical polymerization. Electrochemically active groups are either incorporated into the polymer structure inside the chain or included as a pendant group (prefunctionalized polymers),

added to the polymer phase during polymerization, or fixed into the polymer network in an additional step after the coating procedure (post-coating functionalization) in the case of polymer film electrodes. The latter approach is typical of ion-exchange polymers. The electrochemical polymerization is preferable, especially if the polymeric product is intended for use as a polymer film electrode, thin-layer sensor, in microtechnology, *etc.*, because potential control is a prerequisite for the production of good-quality material and the formation of the polymer film at the desired spot in order to serve as an anode during synthesis. A chemical route is recommended if large amounts of polymer are needed.

Electropolymerization

In the majority of cases the polymers are prepared by electrooxidation of the respective monomer compound. The oxidation of the monomer results in the formation of a cation radical. The chain propagation occurs via dimerization of the radicals formed and elimination of hydrogen ions. The dimer is oxidized (more easily than the monomer) and a next coupling step takes place with a monomeric cation radical. The radical cation—radical cation coupling (RR coupling) –due to the strong Coulombic repulsion– is considered less likely than the radical cation—substrate coupling (RS coupling), *i.e.*, the coupling of a charged and a neutral species. However, in condensed phase RR coupling can proceed in a substantial rate. The nature of the rate-determining step (rds) depends on the conditions; since the rate of the deprotonation, the solubility of the oligomer, the stability of the cation radical depend on the nature of the solvent (*e.g.*, its effect on the proton elimination), electrolyte (especially on the nature of the anion which may stabilize the cation), and temperature [2, 25, 26]. One has to consider also the deposition step which strongly depends on the nature of the substrate (metal, carbon *etc.*). Some metals can catalyze the oxidation of the monomer or a first layer of monomers may be formed due to the chemisorption on the metal which is characteristic in several monomers on Pt or PtO [27].

During the very first potential cycle a characteristic loop (a crossing pattern that appears in the cyclic voltammogram on reverse scan) (Fig. 3) can be observed which is due to the energy needed for the nucleation. According to another view in some cases the loop is due to a homogeneous comproportionation reaction [25] which facilitates the oxidation of the monomer.

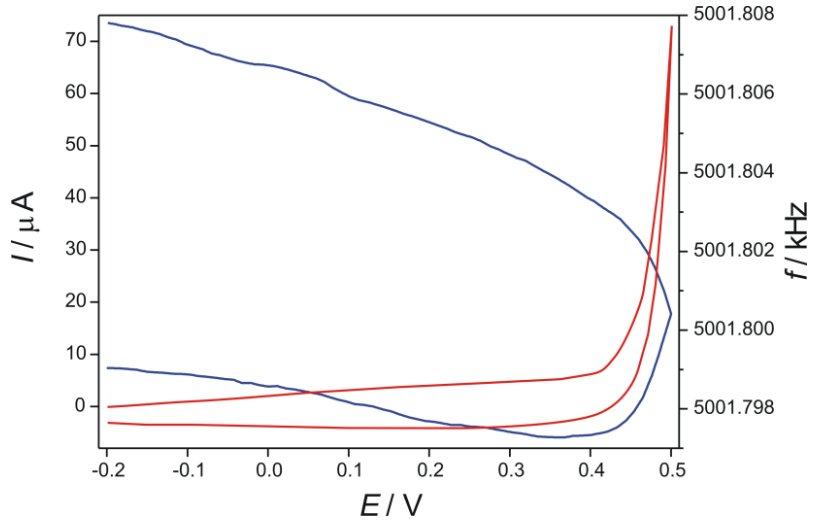

Figure 3. *The 1st cyclic voltammogram (–) and the simultaneously detected EQCN response (–) during the electrooxidation of 6-aminoindole (1.5 × 10^{-2} mol dm^{-3}) on Au in 1 mol dm^{-3} H_2SO_4 solution. Scan rate: 25 mV s^{-1}, switching potential: 0.5 V [27].*

A huge anodic current appears and simultaneously the EQCN resonant frequency starts to decrease which continues until anodic current flows. This indicates a deposition of the oxidation product on the gold surface. The –5 Hz frequency decrease corresponds to a ca. 0.7 nm thin film, assuming 1.2 g cm^{-3} for the density of the film or a surface concentration of 6-aminoindole, Γ = 6.7 $\times$ 10^{-10} mol cm^{-2}. It follows that barely a monolayer or even submonolayer film was formed, *i.e.*, it can be considered just a nucleation. While the nucleation process is somewhat hindered, the growth of the film is a much faster process. In Fig. 3 the so-called nucleation loop, *i.e.*, the crossing pattern of the anodic current and the current after switching is not well seen, because the switching potential was limited to 0.5 V in order to avoid the overoxidation. However, it exists, and well-seen when a higher positive switching potential was applied during the first scan. It has been interpreted as the start of the nucleation process.

The progress of the electropolymerization and the deposition of the polymers can be nicely seen on the cyclic voltammograms since the peak currents (and the charge under the waves) related to the redox responses of the conducting polymer increases. By using electrochemical quartz crystal nanobalance the increase of the deposited mass can be monitored directly. It can be seen in the following figures (Fig. 4 polyaniline, Figs. 5-7 polyindole and poly(4-aminoindole, respectively).

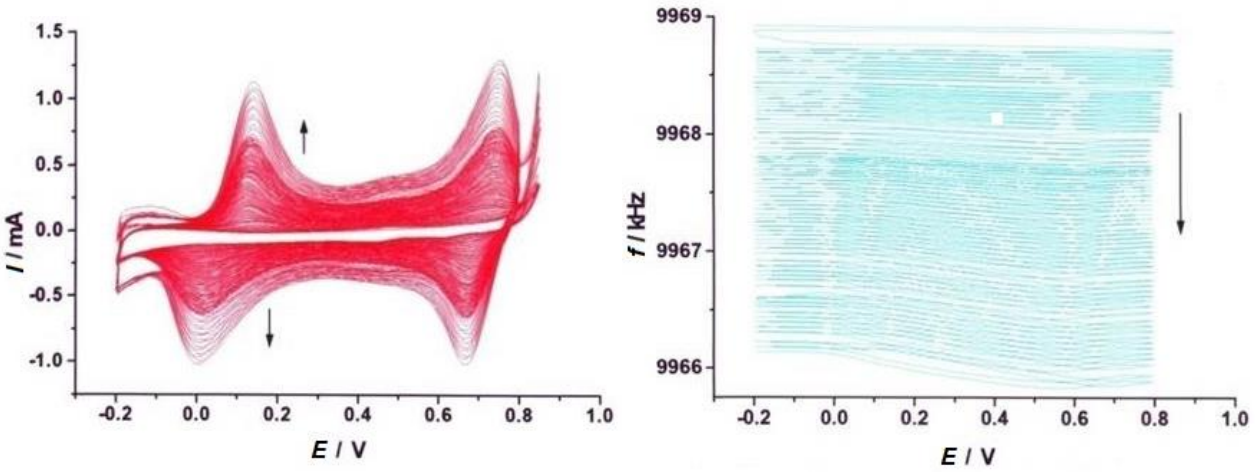

Figure 4. *The cyclic voltammograms and the simultaneously detected EQCN frequency changes during the electropolymerization of aniline at a platinum electrode. Scan rate: 100 mV* s^{-1}*. Solution composition: 0.2 mol* dm^{-3} *aniline in 1 mol* dm^{-3} $HClO_4$ *[28].*

The mechanism of polyaniline formation is influenced by the deposition of oligomers, and the highest growth rate in cyclic electropolymerization occurs during the cathodic potential scan. The film morphology (compactness, swelling) is strongly dependent on the composition of the solution, notably on the type of counter-ions present in the solution, and the plasticizing ability of the solvent molecules. Due to the autocatalytic nature of the electropolymerization, the positive potential limit of cycling can be decreased after 2–10 cycles, which is a common practice used to avoid the degradation of the polymer due to the hydrolysis of the oxidized polyaniline (pernigraniline form). The head-to-tail coupling that results in the formation of *p*-aminodiphenylamine, tail-to-tail dimerization (benzidine) also occurs; however, the latter is considered to be a minor dimer intermediate because the rate constant of dimerization for RR coupling that produces the former product is about 2.5 times higher than that for the tail-to-tail dimer. Two types of nucleation (instantaneous and progressive) and three types of growth (1-, 2-, and 3-dimensional) have been observed in the case of different polymers and conditions. Although the region close to the electrode surface exhibits a more or less well-defined and compact structure, in general the polymer

layer can be considered to be an amorphous material with decreasing density as a function of the distance of the substrate.

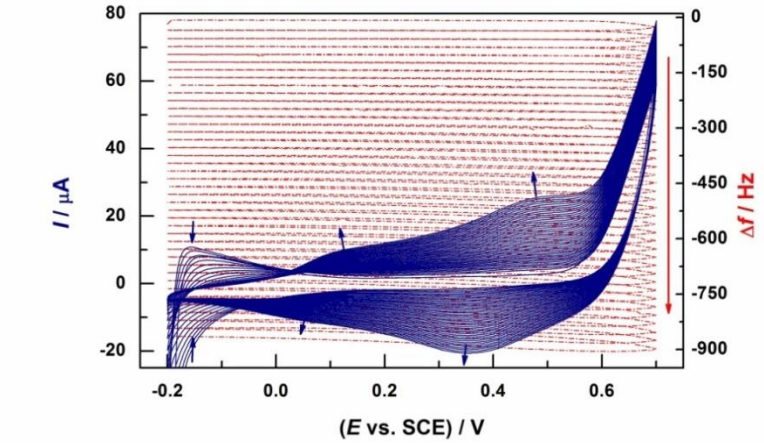

***Figure 5**. Cyclic voltammograms and the simultaneous change of the EQCN frequency (Δf) during the oxidative electropolymerization of indole (1 mmol dm^{-3}) in 1 mol dm^{-3} $HClO_4$ on Pt during 40 consecutive cycles. Scan rate: 10 mV s^{-1} [29]*

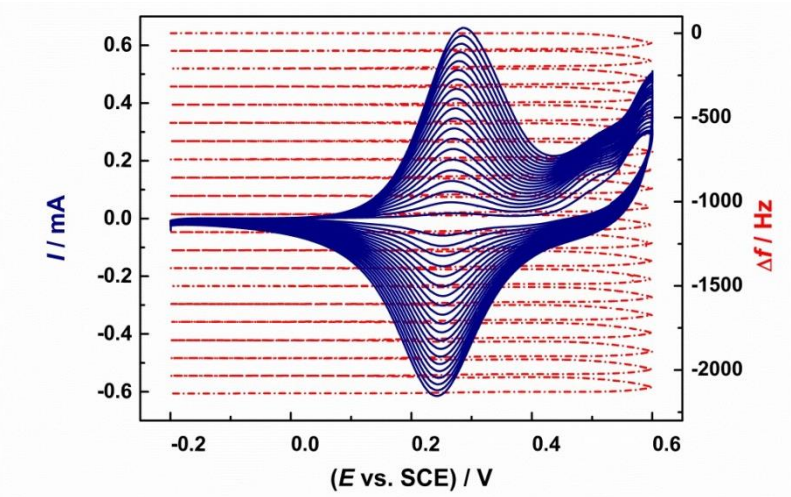

***Figure 6.** Cyclic voltammograms and the simultaneous change of the frequency (Δf) during the electropolymerization of 4-aminoindole (1 mmol dm^{-3}) in 1 mol dm^{-3} $HClO_4$ on Pt, during 20 consecutive cycles. Scan rate: 10 mV s^{-1} [29]*

While the usual representation, *i.e.*, the decrease of the EQCN frequency (or the increase of the surface mass) during consecutive voltammetric cycles can be found in the majority of papers (Figs. 5 and 6), displaying the variation of the EQCN frequency as a function of time can be more instructive. In this case the changes in the course of each cycle are much better seen (Figs. 7). It is well seen that while the surface mass increases from cycle to cycle (continuous decrease of the frequency at the beginning of the subsequent cycles), there is a change during each cycle. In the case of indole this change is getting higher and higher (Fig. 7a) since during the oxidation and reduction counter-ions enter and leave the surface film, respectively, and as the film is getting thicker more and more counter-ions (in this case anions) enter or leave the film in the charge-compensating process. In the case of 4-aminoindole the Δ*f vs.* time curve resembles a staircase (Fig. 7b). This dependence reflects that the deposition occurs with the same rate from cycle to cycle and the frequency variation is independent of the film thickness. It is only possible if there is no movement of ions of considerable mass, *i.e.*, the transport of H^+ ions should be considered instead of anions.

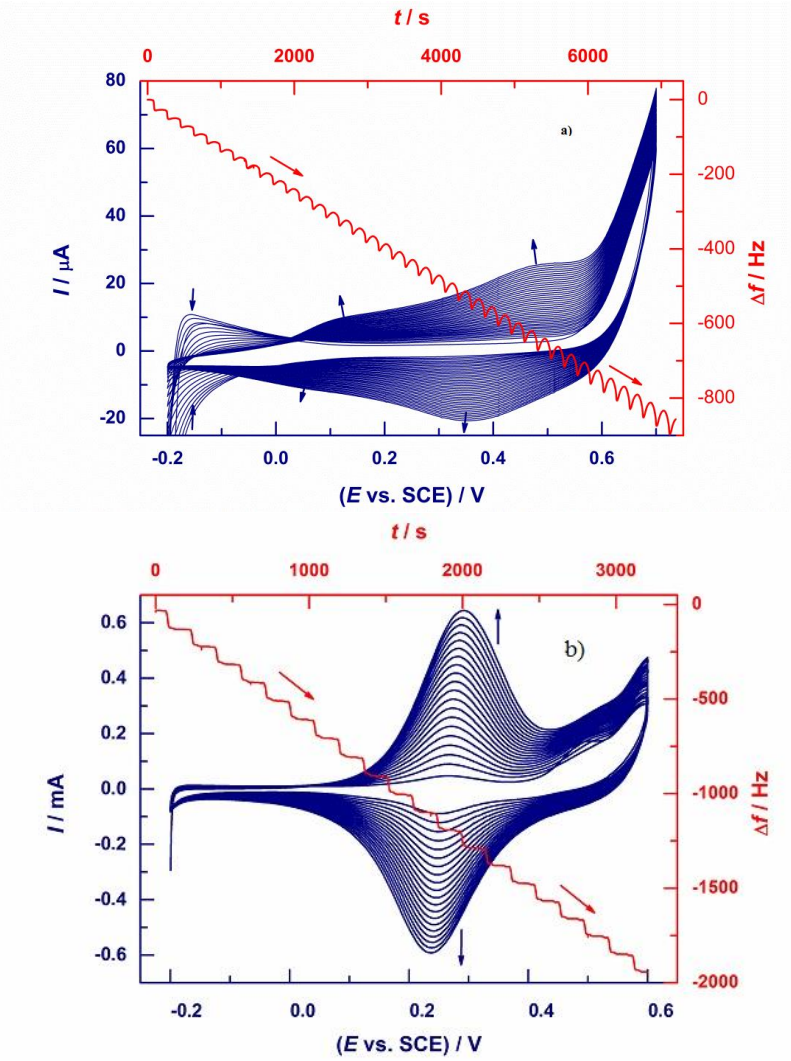

Figure 7. *Comparison of the electropolymerization of indole (a) and 4-aminoindole (b) under the same circumstances on the same type of electrode (1.37 cm^2 Pt) in 40 and 20 cycles, respectively. Cyclic voltammograms and the simultaneously detected frequency curves. The frequency curves are plotted as function of the time. $c_{monomer}$ = 1 mmol dm^{-3}, electrolyte: 1 mol dm^{-3} $HClO_4$. Scan rate: 10 mV s^{-1} [30].*

While electrochemical impedance spectroscopy has become a basic tool in the study of the rate of charge transport processes, film resistances and capacitances of polymer film electrodes, it is relatively seldom used to follow the electropolymerization process. Figures 8 and 9 show such results and the respective electrical equivalent circuit [30].

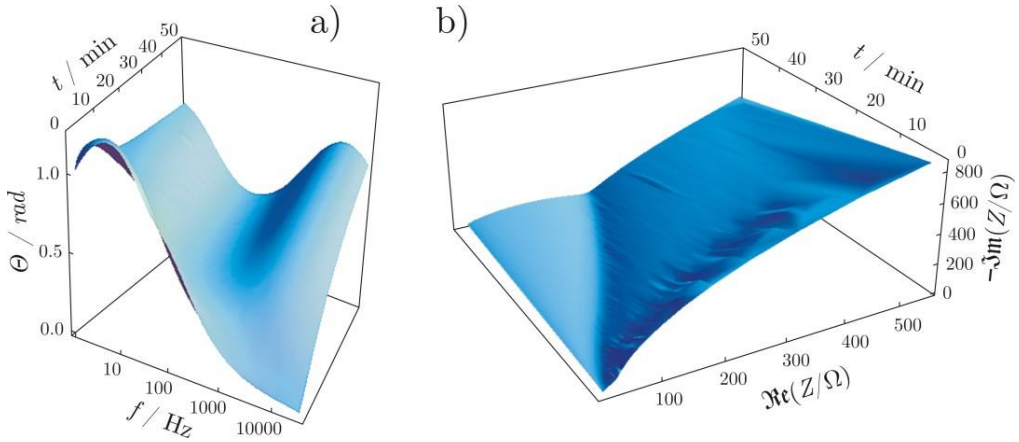

Figure 8. *Three-dimensional representation of the (a) Bode and (b) Nyquist plots of the measured impedance data during the electrodeposition of polyindole on Pt at 0.7 V in 0.1 mol dm^{-3} H_2SO_4 solution [31]*

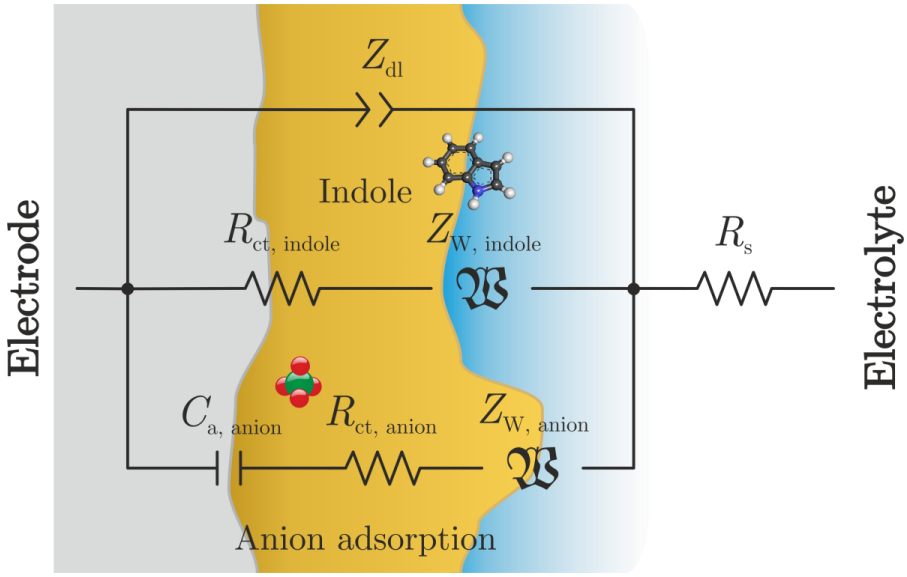

Figure 9. *Electrical equivalent circuit describing the EIS response of polyindole deposition on platinum. Z_{dl} represents the impedance of the double layer, $R_{ct,indole}$ and $Z_{W,indole}$ are the charge transfer and diffusional impedances of indole, respectively, $C_{a,anion}$ is the capacitive impedance related to the counter-ion adsorption (on Pt surface), $R_{ct,anion}$ is the charge transfer resistance associated with the counter-ion adsorption/desorption, $Z_{W,anion}$ is the diffusional impedance of the counter-ions, and R_s is the solution resistance. The equivalent electric circuit has been elucidated based on a priori chemical knowledge about this system [31].*

Following the variation of the characteristic parameters several conclusions could be drawn concerning the events at the surface (adsorption of indole and ions, polymerization *etc.*). The charge transfer resistance and Warburg coefficient associated with indole itself vary with time, providing evidence that after an inductive period, the process of generation of active centers is at its maximum contributing to noticeable diffusion limitations. The apparent rate coefficient reflects the relative contribution of slow and fast electrochemical stages involving the interfacial charge transfer during the film growth. In general, formation of nuclei of a new phase is considerably slower than their growth. At higher times the surface of Pt is covered by the polymer film, so that the growth at the Pt/polyindole boundary is suppressed. However, the diffusion coefficient of the indole molecules in/at the relatively thick indole film is decreased. The sulfate adsorption capacitance significantly changes during the polymer film growth. At the anodic potential selected for polymerization, it is known that the sulfate surface coverage is ~0.2 monolayer (ML) in H_2SO_4, and the adsorption capacitance is approximately a few μF cm^{-2} as the adsorbate layer is almost "saturated". After 5 min of indole electropolymerization, the adsorption capacitance increases up to ~200 μF cm^{-2}. This value roughly corresponds to 0.1 ML of sulfates adsorbing and desorbing during the low-amplitude ac probing, *i.e.* ~50 % of the available adsorbed sulfates are "disturbed" during initial stages of polymerization. However, after ~10 min, the adsorption capacitance decreases (~100 μF cm^{-2}) and remains approximately constant. The non-zero values of the adsorption capacitance after ~10 min indirectly suggest that redox transformations at the polymer/Pt interface still significantly disturb the adsorbed sulfate layer.

Overoxidation

The overoxidation is a general problem in the course of the electropolymerization and also the investigation or the use of conducting polymer modified electrodes. The choice of positive potential limit in the case of electropolymerization or the application of proper oxidant (redox couple which does not possess too positive equilibrium potential) in the case of chemical oxidation is essential to

have a good quality polymer. At high anodic potentials the further oxidation of the polymer occurs, and this oxidation product undergoes a chemical reaction, *e.g.*, in the case of polyaniline quinone groups appear due to hydrolysis reaction. It manifests itself in the so-called "middle peak" between the two main voltammetric peaks (see Fig. 10).

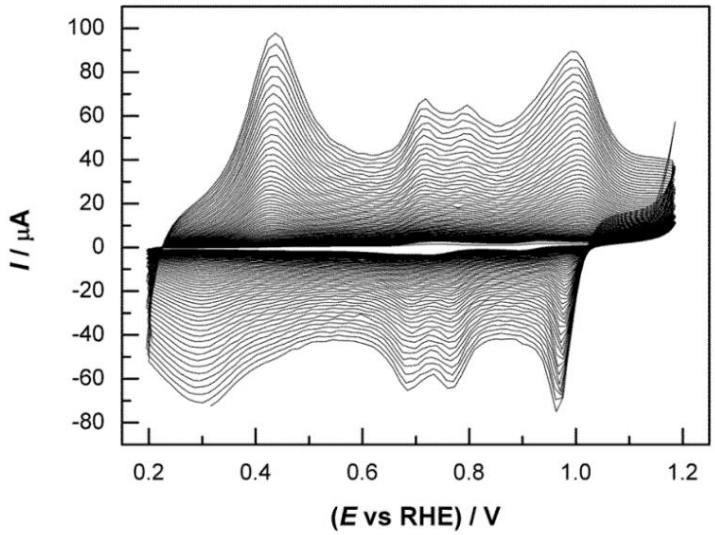

Figure 10. *The consecutive cyclic voltammograms during the electropolymerization of aniline at a platinum electrode. Scan rate: 100 mV s^{-1}. Solution composition: 0.2 mol dm^{-3} aniline in 0.5 mol dm^{-3} H_2SO_4*

In the case of the electropolymerization of 4-aminoindole it can be seen that during the consecutive cyclic voltammograms (2-6th and 7-9th) the current continuously decreases during the cycling together with a shift of the peak potential. The rate of the frequency change shows also decreasing characteristics from cycle to cycle (Fig. 11). By using positive potential limits above 0.6 V an overoxidation and hydrolysis occur and the electroactivity and conductivity of the film become negligible. Nevertheless, a bluish-purple layer, which was formed, remained on the surface. Similar phenomenon can be observed practically for all indole derivatives as shown in Figures 12-14 in the case of 6-aminoindole.

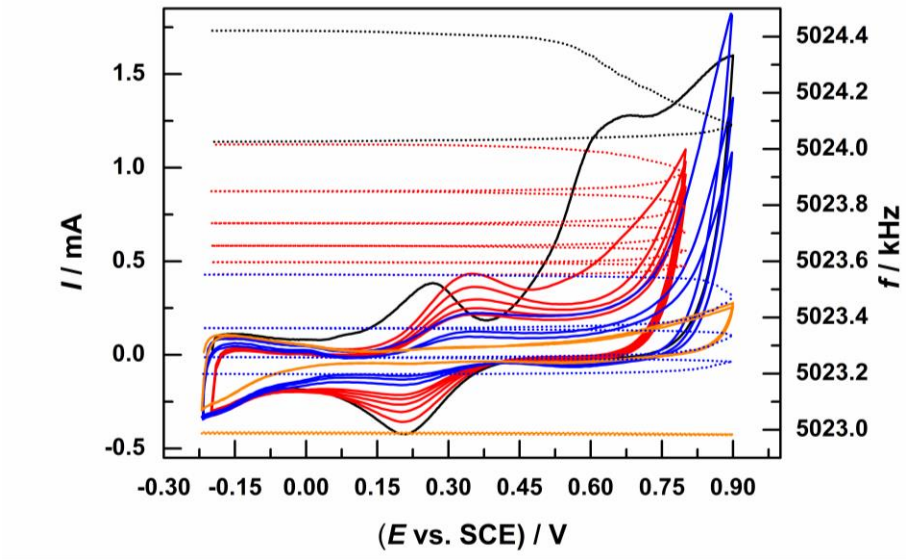

Figure 11*. Effects of the extended positive potential limit. The figure shows the first cycle (black), from the 2nd to the 9th cycle (red), and the 19th and 20th cycles (yellow) from a series of measurements. Solution: 1 mmol·dm^3 4-aminoindole in 0.5 mol·dm^3 H_2SO_4. Pt electrode, v = 20 mV·s^1 [29].*

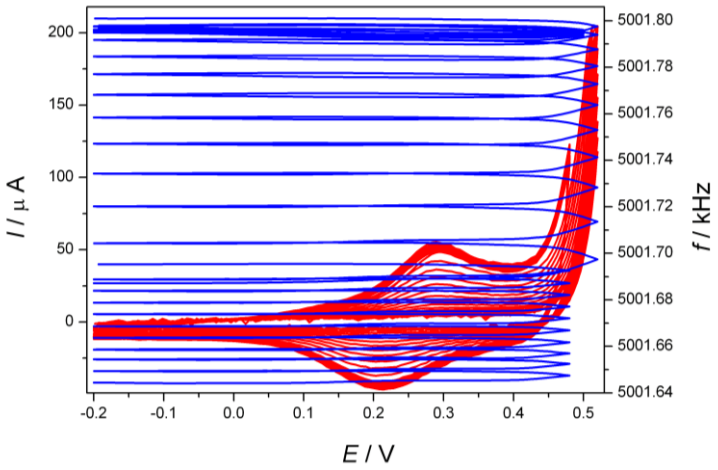

Figure 12. *Subsequent cyclic voltammograms and the simultaneously detected EQCN responses during the electrooxidation of 6-aminoindole (1.5 × 10^{-2} mol dm^{-3}) on Au in 1 mol dm^{-3} H_2SO_4 solution. Scan rate: 25 mV s^{-1}. After the 17th cycle the switching potential was decreased to 0.48 V [27]*

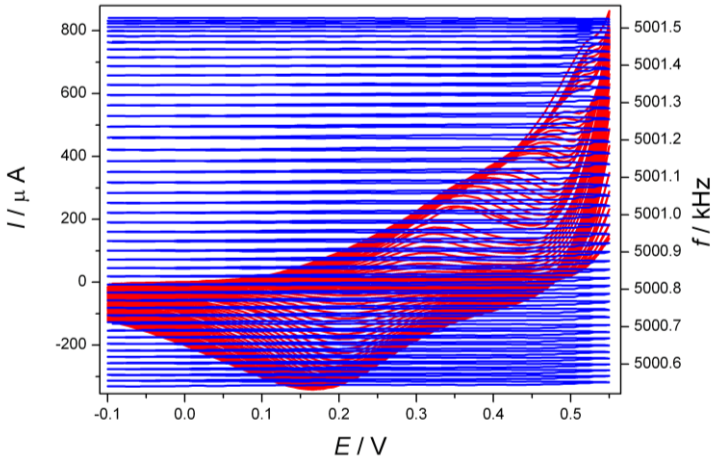

Figure 13. *Subsequent cyclic voltammograms and the simultaneously detected EQCN responses during the electrooxidation of 6-aminoindole (1.5 × 10^{-2} mol dm^{-3}) on Au in 1 mol dm^{-3} H_2SO_4 solution. Scan rate: 50 mV s^{-1}. The first 46 cycles between –0.1 V and 0.55 V without changing the switching potential [27].*

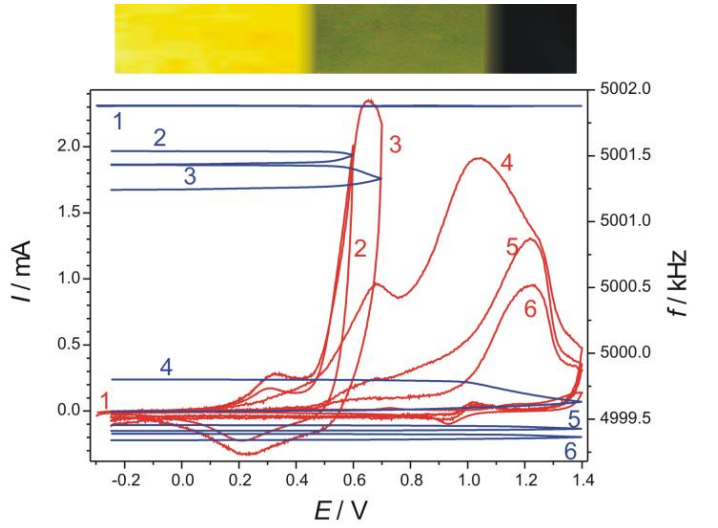

Figure 14. *Cyclic voltammograms and the simultaneously detected EQCN responses during the electro-oxidation of 6-aminoindole film on Au in contact with 1 mol dm^{-3} H_2SO_4. The change of the color of the film by using the original photos of the electrode is also displayed. The positive potential limit was increased during the consecutive cycling. The responses of the clean gold electrode in the potential range between –0.3 V and 1.40 V (1). Positive potential limits were as follows: 0.55 V (2), 0.65 V (3), and 1.4 V (4-6) (three subsequent cycles) [27].*

The oxidation peak of the polymer, appearing at 0.27 V in the course of the first cycles when 0.5 V potential limit was kept, gradually shifts into the direction of more positive potentials. Its height shows decreasing tendency with cycling to higher positive switching potentials (curves 2-4 of Fig. 14). The oxidation peak of the monomer appears at 0.6 V, the frequency decrease related to the deposition of the polymer gradually increases (curves 2 and 3 of Fig. 14). During continuous cycling using higher and higher positive potential limits the deposited mass increases. However, the peak height and the charge consumed during the oxidation of the monomer (together with the oxidation of the film) decreases, and eventually both the charge and the frequency observed earlier by applying a given switching potential gradually diminishes (for the sake of clarity not all cycles are shown in Fig. 14). When 1.4 V switching potential was applied (curves 4-6) the effect described above is well seen. Finally, during cycling 7 Hz frequency variation can be observed, which is approximately equal to the magnitude of the usual double layer charging, *i.e.*, no further deposition takes place, and the film redox activity also diminishes. Nevertheless, a bluish-purple layer, which was formed, remained in the surface. Because of the loss of electrochemical activity it can be concluded that the conjugated polymer bonds break down, and an indigo or indirubin-like insoluble but colored layer is formed.

Thermodynamical considerations

Thermodynamical considerations (the question of equilibria)

No equilibrium (adsorption equilibrium) exists between the surface phase and the solution with respect to the polymer. In most cases no chemical bonds exist between the substrate and the polymer, the polymer layer remains at the surface due to the van der Waals forces between the substrate and the polymer, as well as between the polymer chains in multilayer films. The adsorption model of de Gennes predicts a diminishing layer density which has been observed, indeed, *i.e.*, the polymer film is more compact close to the substrate surface.

Equilibrium situation is seldom established within the time scale of the experiments since the relaxation process of the polymer network (gel) may be extremely long. It is true not only with respect to the polymer morphology (conformation) but also to the membrane equilibria with participation of ions and solvent molecules. In the first approach the surface polymer layer can be treated as an amorphous swollen gel with a uniform structure and density in contact with a solution containing solvent molecules and ions. In this case, both non-osmotic and osmotic membrane equilibria, as well as the mechanical work done in swelling the polymer, must be taken into account. In most cases the situation is even more complicated than that usually treated using membrane equilibrium, since the charge in the polymer changes during the redox reaction; in most cases a neutral polymer is transformed into a polyelectrolyte, and vice versa.

Membrane equilibria

Even in the case of a neutral polymer one should consider the partitioning equilibria of the solvent molecules, the neutral salt and the ions formed by dissociation. The solvent content in the polymer phase obviously depends on the difference between the standard chemical potentials of the solvent molecules in the two contacting phases. Ions enter the film if their van der Waals and ion-dipole interactions with the polymer are large. Ions can be solvated (hydrated) by both the polymer and the solvent. When the polymer is hydrophobic and the solvent is hydrophilic the interaction energies between the polymer segments and between the solvent molecules are higher than those between the polymer segments and the solvent molecules. In this case, the polymer

segments are not solvated by the solvent molecules, and hence there is no solvent swelling of the polymer film. If the neutral polymer contains polar groups, water molecules will enter the polymer and the polymer phase will eventually contain substantial amounts of water.

The situation is different when the interface is not permeable for one of the ions; *i.e.*, the polymer film behaves like an ion-exchange membrane. This is the case when the polymer is charged, which is usually achieved by oxidation or reduction; however, this can also be the result of protonation. Two cases should be considered: (i) non-osmotic membrane equilibrium; (ii) osmotic membrane equilibrium. In the latter case, where solvent molecules can enter the surface layer or the membrane, the situation is more complicated since mechanical equilibria are also involved. The non-osmotic membrane equilibrium is illustrated in Fig. 15.

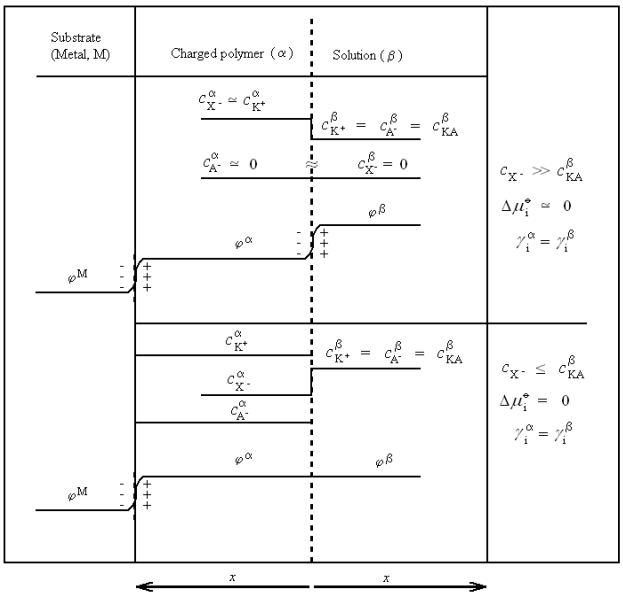

Figure 15*. Charged polymer in contact with an electrolyte solution. Non-osmotic membrane equilibrium [2]*

In the case of osmotic membrane equilibrium incorporation of ions and solvent molecules into the polymer phase, a swelling of the polymer layer occurs, *i.e.*, the state of the polymer phase depends on the potential. For the thermodynamical description of the expansion or contraction of the polymer network a mechanical work term has to be considered. The deformation of the polymer layer: plastic (break-in period) or elastic (reversibly coupled to the redox reaction).

Redox transformations and the accompanying processes

The electron transfer taking place at the metal|polymer interface is accompanied by ionic charge transfer at the polymer|solution interface, in order to maintain the electroneutrality within the polymer phase. Counter-ions usually enter the polymer phase. However, less frequently the electroneutrality is established by the movement of co-ions present in the polymer phase, *e.g.*, in so-called "self-doped" polymers. Oxidation reactions are often accompanied by deprotonation reactions, and H^+ ions leave the film, removing the excess positive charge from the surface layer. It should also be mentioned that simultaneous electron and ion transfer is also typical of electrochemical insertion reactions; however, this case is somewhat different since the ions do not have lattice places in the conducting polymers, and both cations and anions may be present in the polymer phase without any electrode reaction occurring. A general scheme of the charge transport and the accompanying processes is shown in Fig. 16.

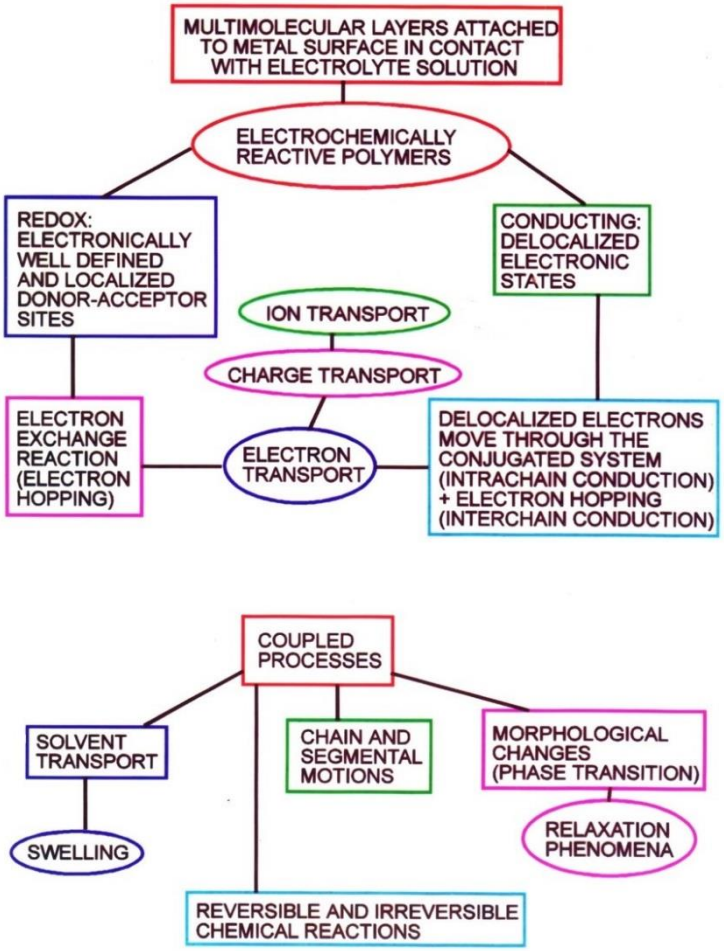

Figure 16*. The charge transport and the accompanying processes in the case of a polymer film electrode*

Owing to the complexity of the system and its redox transformations to gain a deeper understanding of the mechanism combined techniques should be applied. In many cases even the combination of more techniques is necessary. Two examples will be presented below. The considerable difference between the anodic and cathodic peak potentials of the cyclic voltammograms for the poly(tetracyanoquinodimethane) (TCNQ) redox electrode has been explained by the formation of dimeric species; *i.e.*, the slow formation of mixed-valence dimers during reduction (charging) and the fast re-oxidation of dimer dianions resulting in mixed-valence dimers during the discharging process [31]. The concentrations of the anion radicals and the dimer dianions were derived from UV-VIS spectroelectrochemical data. The concentration of the mixed-valence dimer was calculated from the variation in the ESR intensity and the concentration of the other paramagnetic species, $TCNQ^{\cdot-}$ and $TCNQ^{\cdot-}_2$ (Fig. 17). It is striking evidence that even UV-VIS spectroelectrochemistry is not enough to reveal all the intermediate products since the mixed-valence dimer, $TCNQ^{\cdot-}_2$ is silent within the available spectral lengths.

In order to monitor the transport and equilibria of ions and solvent molecules the electrochemical quartz crystal nanobalance (EQCN) and radiotracer techniques are relatively simple but highly effective methods. A comparison of the behavior of polyindole and poly(4-aminoindole) serves as an illustration (Figures 18 and 19).

The reduction peak belonging to the first oxidation peak is rather undeveloped and suppressed by the second one. The frequency change follows the charging–discharging processes. The apparent molar mass, that corresponds to the $\Delta f/Q$ quotient is 90.6 g mol^{-1} (n = 1). Therefore, ClO_4^--anions enter and leave the film during its oxidation and reduction, respectively.

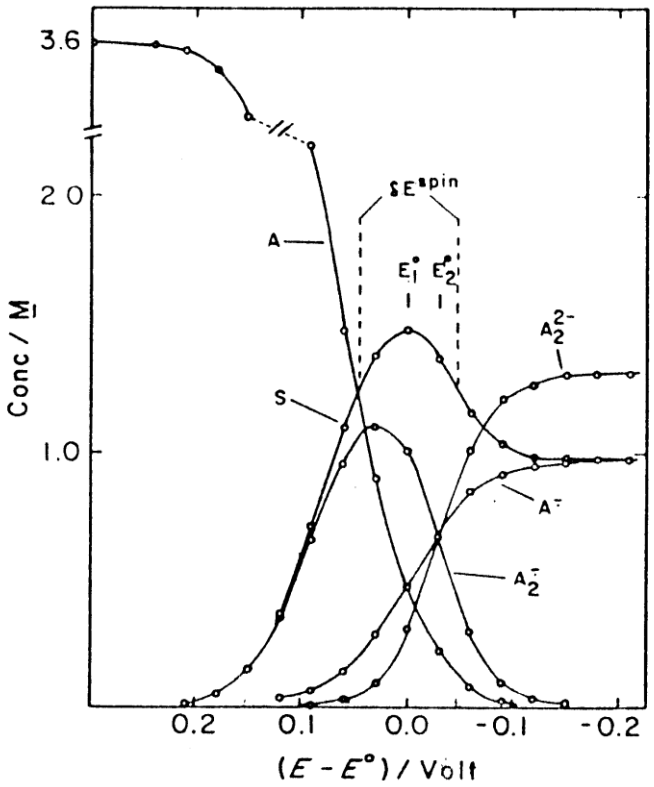

***Figure 17**. Distribution diagram for the species formed during the electroreduction of poly(tetracyanoquinodimethane). A = TCNQ, A^- = $TCNQ^-$, A_2^- =$TVNQ_2^-$, A_2^{2-}=$TCNQ_2^{2-}$, and S = c_{TNCQ^-} + $c_{TNCQ_2^-}$ [32]*

In the case of poly(4-aminoindole) based on the frequency change vs. potential curve three processes can be distinguished in both scan directions (Fig. 19).

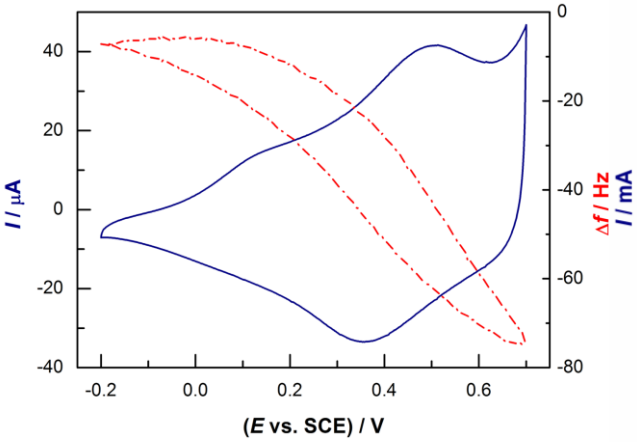

***Figure 18.** Cyclic voltammogram with the frequency change curve of a polyindole film in 1 mol dm^{-3} $HClO_4$. Scan rate: 10 mV s^{-1} [29]*

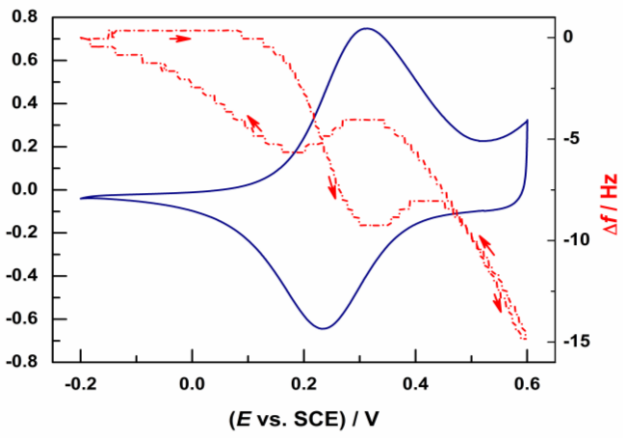

***Figure 19**. Cyclic voltammograms and the corresponding frequency curves of a poly(4-aminoindole) layer on Au, measured in (1 mol dm^{-3} $HClO_4$) at 10 mV s^{-1} [29]*

In the positive scan direction, from 0.1 V an increasing current can be detected. Simultaneously a mass increase starts, which is attributable to anion incorporation. However, the apparent molar mass value (M = 10 g mol^{-1}) that can be calculated from the mass vs. charge function is much lower than the molar mass of the perchlorate ions. While the frequency decrease during the ascending part of the cyclic voltammetry wave is evident, its value is rather small especially compared to the relatively substantial charge consumed. This observation can be elucidated by assuming simultaneous anion sorption and deprotonation, and the latter process is the dominant one. Together with

protons water molecules also leave the film, *i.e.*, desorption of hydrated H_3O^+ can be considered. From 0.3 V, a strange frequency increase-decrease pattern can be detected before the next frequency decrease section. This type of changes has been detected in the cases of other systems, and has been assigned to a structural rearrangement which occurs simultaneously with a partial deprotonation and dehydration of polymer layer. Further charging results in anion incorporation and deprotonation again. The EQCN technique can resolve the events occurring under the wide voltammetric wave, and these results reveal that the charge compensating processes are more complicated than that are usually expected. Therefore, at least three consecutive processes can be considered despite the single pair of peaks that appears in the current response.

A direct way to monitor the ion exchange processes can be achieved by radiotracer technique. Using the radiotracer method, the strength of the ion–polymer interactions can also be studied, which is certainly a special advantage of this technique. When unlabeled species are added to the solution phase in great excess, the sorbed species are exchanged provided that there are no strong interactions (chemical bonds) between the ions or molecules and the polymer. At a given potential the mobility of the ions can be tested (Fig. 20).

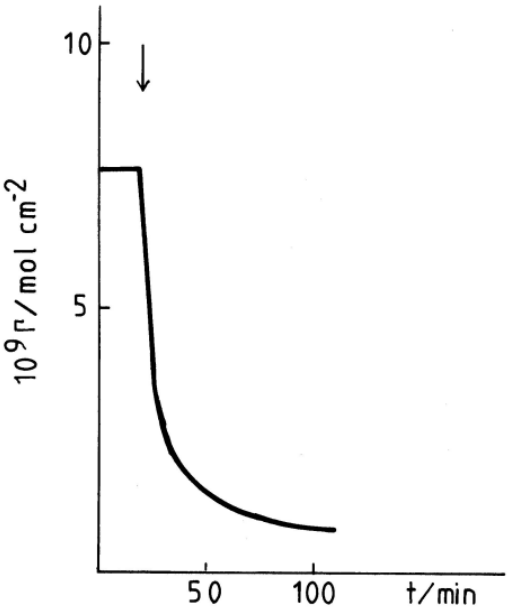

Figure 20*. The exchange of labeled SO_4^{2-} ions sorbed in polypyrrole film with unlabeled SO_4^{2-} ions added to a solution phase containing 10^{-5} mol dm^{-3} ^{35}S-labeled H_2SO_4 and 10^{-2} mol dm^{-3} $HClO_4$ at the moment indicated by the arrow. E = 0 V. Final H_2SO_4 concentration: 2×10^{-2} mol dm^{-3} [33]*

The results presented in Fig. 20 attest that ions embedded in polypyrrole (PP) film are mobile, despite the fact that the interactions between PP and SO_4^{2-} are much stronger than those between PP and ClO_4^- ions, since ClO_4^- ions are present at a concentration that is three orders of magnitude greater.

The periodical sorption/desorption of Cl^- ions during four consecutive potential cycles in the case of a polypyrrole electrode can be seen in Fig. 21. As expected Cl^- ions enter the PP film during oxidation and leave it during reduction.

A comparison of the data obtained by radiotracer and piezoelectric nanogravimetric techniques (EQCN) is especially useful, because the latter supplies information on the total surface mass change due to the deposition or sorption of different species, while the contributions originating from the different species can be unambiguously separated by labeling the respective molecules or ions.

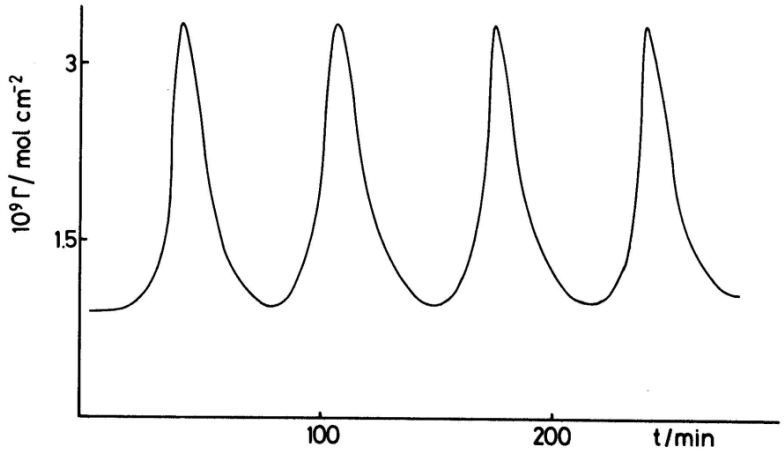

***Figure 21**. The change in the amount of Cl^- ions in a polypyrrole electrode during four consecutive oxidation--reduction cycles. Solution: 2×10^{-4} mol dm^{-3} ^{36}Cl-labeled HCl. Scan rate: 0.4 mV s^{-1}. [33]*

Recently, a new software controlled electrochemical measuring system for the simultaneous measurements of surface mass changes and optical absorbance spectra has been developed [34]**.** By using an EQCN, extremely useful quantitative information about electrode processes such as adsorption, deposition and dissolution, ion and solvent exchange between the surface film and the solution can be obtained. However, by using EQCN only the total mass change can be measured even in the case of ideal behavior. Therefore, one can draw reliable conclusion concerning the mechanism, if the nature of the intermediates and products of the electrochemical reactions will be determined by an independent technique. If the formed products or intermediates are colored species, spectroelectrochemistry is a plausible choice. The simultaneous use of the EQCN technique with spectroscopic UV-VIS measurements certainly helps to solve this problem (Fig. 22)**.**

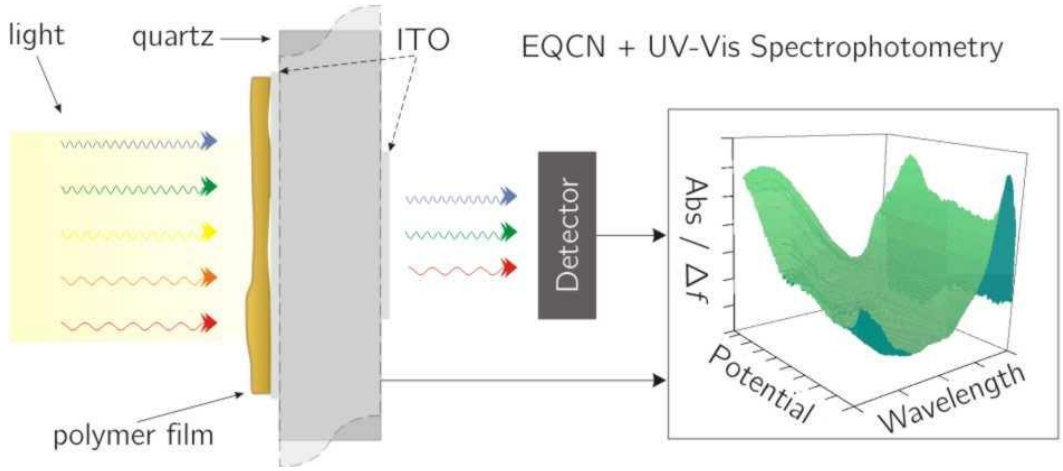

***Figure 22**. Absorbance of the polyaniline layer during a single anodic potential scan. Bare ITO crystal was taken as reference. Scan rate: 10 mV s^{-1}, electrolyte: 0.1 mol dm^{-3} H_2SO_4, $c_{aniline}$ = 0.01 mol dm^{-3} [34]*

Polymeric (polyelectrolyte) properties

Effect of temperature. Difference between redox and conducting polymers

The increase of temperature enhances the chain and segmental motions, therefore a more reversible, surface cyclic voltammetric behavior can be observed due to the more effective electron transport (Fig. 23). Of course, the rate of the counter-ion's motion also increases, however, in the case of redox polymers the polymeric motion and consequently the rate of the electron hopping is usually the rate-determining process.

In the case of intrinsically conducting polymers usually the intrachain electron transport is dominating, and consequently the temperature has no or a minor effect on the cyclic voltammograms (Fig. 24). Albeit in the case of polyaniline at higher pH values a strange effect can be observed, *i.e.*, shift of the voltammetric wave occurring at more positive potentials. It is related to the temperature dependence of the protonation constant of the weak base, therefore similar phenomenon appears with pH variation (Fig. 25).

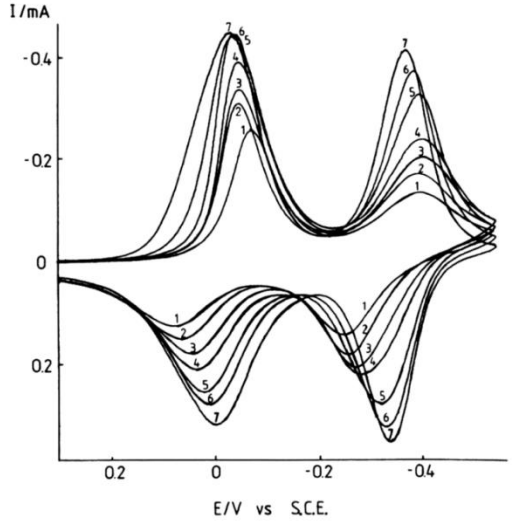

Figure 23*. Cyclic voltammograms of a poly(tetracyanoquinodimethane) (TCNQ) electrode (Γ= 5.1×10^{-8} mol cm^{-2}) in contact with aqueous 10 mol / dm^3 LiCl. Scan rate: 6 mV s^{-1}. Temperatures: (1) 22.5, (2) 34.2, (3) 43, (4) 50.5, (5) 61, and (6) 77 °C [35]*

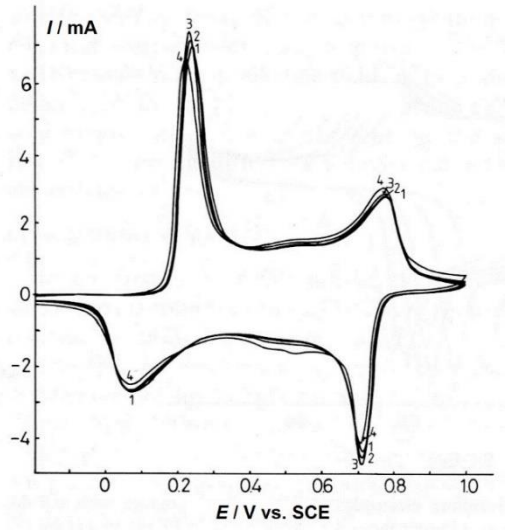

Figure 24. *Temperature dependence of cyclic voltammetric response of a polyaniline film at different temperatures. Temperatures: 1.5 (1), 4 (2), 13 (3) 29 °C (4); 1 mol dm^{-3} HCl pH = 0 v = 60 mV s-^{1} [36]*

The electrochemical responses and also the change of other properties, *e.g.*, color changes remain still fast at rather low temperatures. This is of practical importance because it allows using this system in electrochromic display devices at very low temperatures where the usual displays based on liquid crystals fail (Fig. 26).

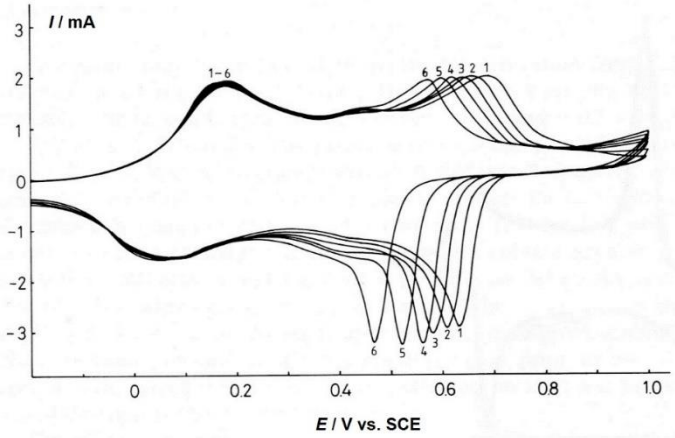

Figure 25. *Temperature dependence of cyclic voltammetric response of a polyaniline film at different temperatures. Temperatures: 19 (1), 29 (2), 36 (3), 46 (4), 58 (5), 66 °C (6); 0.9 mol dm^{-3} Na_2SO_4 mol dm^{-3} + 0.2 $NaHSO_4$ pH = 2.65 (lower part). v = 60 mV s^{-1} [36]*

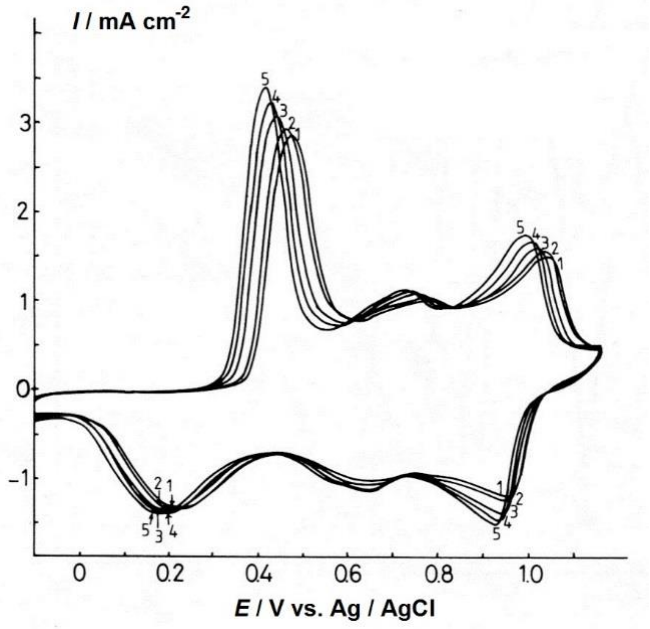

Figure 26. *Temperature dependence of cyclic voltammetric response of a polyaniline film in contact with moist acetonitrile containing 0.1 mol dm^{-3} H_2SO_4, 0.1 mol dm^{-3} tetrabutylammonium perchlorate and 0.01 mol dm^{-3} HCl (water content: 1.5 %) at different temperatures. Temperatures: –42 (1), –36.5 (2), –31 (3), –26.5 (4), and –21 °C (5). v = 25 mV s^{-1} [36]*

Effect of the electrolyte concentration

The swelling and shrinking of a polyelectrolyte gel are strongly affected by the concentration of the contacting electrolyte solution and the temperature. Thermodynamic theory, which considers three contributions to the free energy of the gel (*i.e.*, mixing of constituents, network deformation, and electrostatic interactions), predicts gel shrinkage as the salt concentration is increased. The shrinking process usually occurs smoothly, but under certain conditions the process becomes discontinuous, and the addition of a tiny amount of salt will lead to the collapse of the gel; *i.e.*, a drastic decrease in the volume to a fraction of its original value. These effects have strong influence on the cyclic voltammograms especially in the case of redox polymers (Figs. 27 and 28).

In a more compact structure the rate of electron hopping may increase since the concentration of redox sites is high; however, deterioration in the film's permeability to the counter-ions due to

the decrease in the free volume is expected at the same time. The maximum observed in the peak current versus salt concentration curve is the result of the balanced effects of the enhanced electron-exchange process and the hindered counter-ion motion. The abrupt change in the free volume of solvent-filled cavities causes a sharp decrease in the charge transport diffusion coefficient. A rigorous theoretical treatment which takes into account the extension and contraction of the polymer chain as it is electrochemically converted into a polyelectrolyte is very difficult if not impossible due to the complexity of the polyelectrolyte systems and the lack of an appropriate set of data. These effects were modeled in an empirical approach by scaling the concentration of electroactive sites in the polymer film and the effective charge transport diffusion coefficient (D_{ct}) with $c_s^{1/2}$ [4, 37].

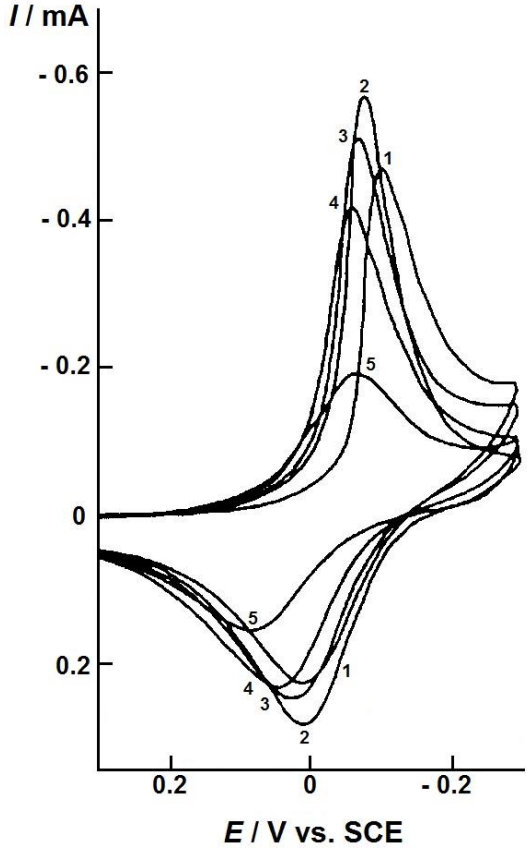

Figure 27. *Cyclic voltammograms of a poly(tetracyanoquinodimethane) electrode in contact with lithium chloride solutions of different concentrations: (1) 0.625, (2) 1.25, (3) 2.5, (4) 5.0 and (5) 10.0 mol dm^{-3}. Scan rate: 60 mV s^{-1} [37]*

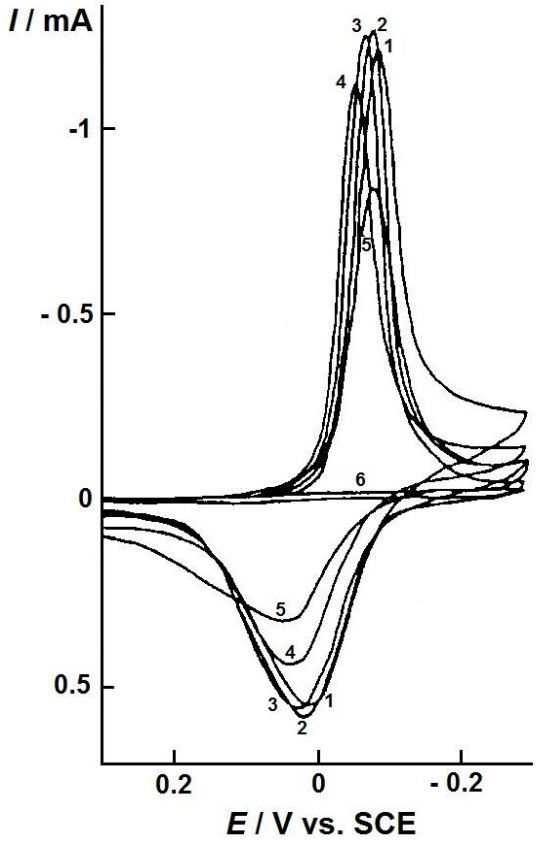

Figure 28. *Cyclic voltammograms of a poly(tetracyanoquinodimethane) electrode in contact with calcium chloride solutions of different concentrations: (1) 0.15, (2) 0.31 (3) 0.625, (4) 1.25, (5) 2.5, (6) 5.0 mol / dm^3 $CaCl_2$. Scan rate: 25 mV s^{-1} [37]*

By employing the empirical equations:

$$c = Z\,(\mathbf{1} + Bc_s^{\mathbf{1/2}}) \tag{1}$$

and

$$D_{ct} = D_{ct}^0(1 - H'c) \tag{2}$$

semi-quantitative description of the effect of concentration on peak currents and peak potentials has been obtained. D_{ct}^{o} is the effective diffusion coefficient of charge transport through the polymer

film in the absence of the addition of supporting electrolyte; *Z*, *B*, and *H′* are empirical parameters characteristic of the system under study. The values of these parameters depend on the nature of the solvent, on the counter-ions (their size and charge), and the polymer forming the film. Combining (1) and (2) with the Randles–Ševčík equation, as well as the appropriate Nernst equation, gives the relationships:

$$I_p = K_i \left[1 - H\left(1 + Bc_s^{1/2}\right)\right]^{1/2}\left(1 + Bc_s^{1/2}\right) \quad (3)$$

and

$$E_p = K_E + \frac{RT}{zF} ln\left\{c_s\left[1 - H\left(1 + Bc_s^{1/2}\right)\right]^{1/2}\right\} \quad (4)$$

where

$K_i = 2.69 \times 10^5 D_{ct}^{o1/2} A v^{1/2} Z$ and $H = ZH'$

$K_E = E_c^{\ominus\prime} - \frac{RT}{zF} ln K \pm 0.0285$.

The constant in the equation of the peak current (K_i) includes the quantities in the Randles–Ševčík equation; *i.e.*, *A* is the electrode area, *v* is the scan rate, and the charge number of the electrode reaction is assumed to be 1. The constant in the equation of the peak potential (K_E) contains the formal potential ($E_c^{\ominus\prime}$) and the formation constant of the salt, ion pair, or complex (*K*). +0.0285 V and −0.0285 V, respectively, have to be used for the anodic and cathodic peak potentials. Where a + or a − sign appears before the term of (*RT* / *zF*) ln*K* depends on the type of ions exchanged. When counter-ions enter the polymer film it is + for reduction and − for oxidation, respectively. For instance, for the reduction of TCNQ the sign is positive. However, when co-ions leave the film, the opposite sign applies, *i.e.*, during oxidation the sign is positive. The most remarkable conclusion of these calculations is the fact that the variation in the I_p and E_p values with c_s can be described with the same set of parameters for a given system. In addition, the variation in *Z*, which is characteristic of the chemical structure of the film, *B*, which in turn is linked to the swelling (solvent–polymer and ion–polymer interactions) and *H*, which expresses how the permeability of the film depends on the sizes of the penetrating ions and the solvent-filled cavities (the free volume in the film), exhibited rather reasonable, systematic changes as the solvent was replaced with a better one or univalent ions were substituted for bivalent ones.

Hysteresis and relaxation phenomena

Despite the quasi-equilibrium character of the cyclic voltammetric curves, a pronounced hysteresis (*i.e.*, a considerable difference between the anodic and cathodic peak potentials) appears. Slow heterogeneous electron transfer, effects of local rearrangements of polymer chains, slow mutual transformations of various electronic species, first-order phase transition due to an S-shaped energy diagram (*e.g.*, due to attractive interactions between the electronic and ionic charges), dimerization, and insufficient conductivity of the film at the beginning of the anodic process have been proposed as possible explanations for the hysteresis (Fig. 29).

Owing to the long relaxation times characteristic of polymeric systems, the equilibrium or steady-state situation is often not reached within the time-scale of the experiment. Fig. 30 shows the change in the resistance of polyaniline after potential steps. The achievement of a constant resistance value takes a rather long time, especially during the conducting-to-insulating transition.

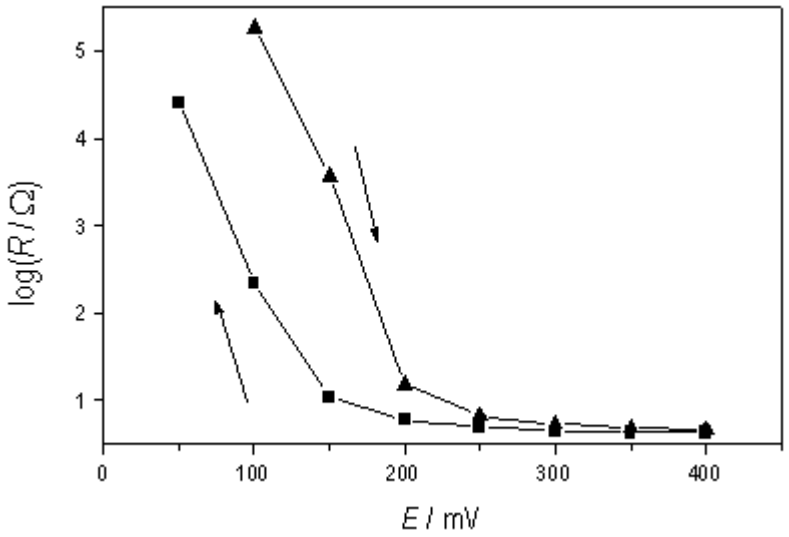

***Figure 29**. The change in the resistance of a polyaniline film in contact with 1 M H_2SO_4 as a function of the potential [7]. Arrows indicate the anodic and cathodic directions of the measurements, respectively*

Consequently, even slow sweep rate cyclic voltammetry does not supply reliable thermodynamic quantities that can otherwise be derived by analyzing the changes in the peak potentials. It is even more striking when the mass change is followed after potential steps. Due to the limited rate of the ion transport and especially the slower solvent transports the constant swelling is achieved often after tens of minutes [38].

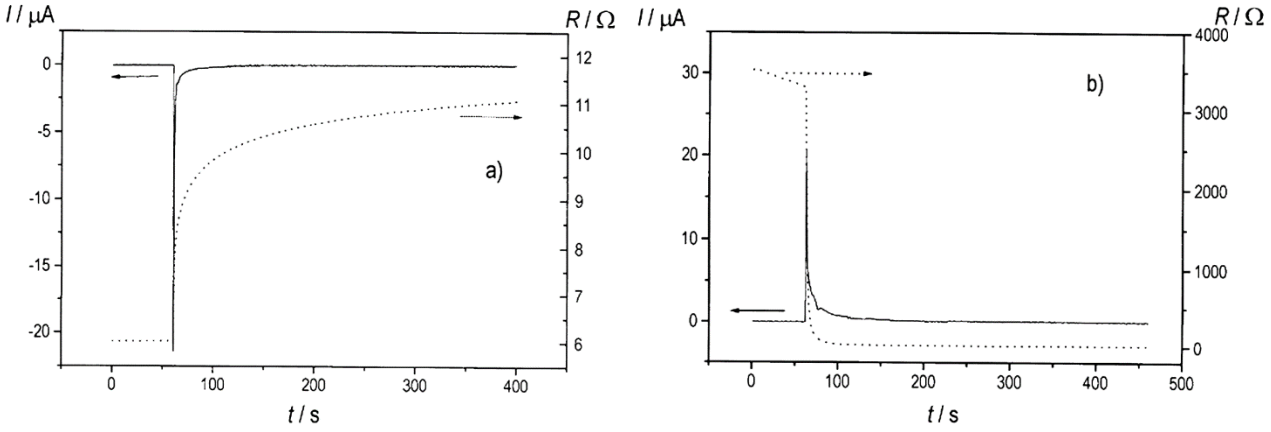

***Figure 30**. The current transients and the respective resistance–time curves obtained after performing potential steps (a) from 0.2 to 0.15 V and (b) from 0.15 to 0.2 V for a PANI electrode in contact with 2 mol dm^{-3} H_2SO_4 [7]*

While the effect of potential-induced relaxation phenomena has been studied extensively, less effort has been expended in exploring the effect of temperature. One notable exception is a temperature shock experiment on a poly(tetracyanoquinodimethane) electrode. It was found that when the electrode returned from elevated temperature to room temperature, a relatively long time (>30 min) was needed to restore the original room-temperature voltammetric response, as seen in Fig. 31.

Apparently, the polymer adopts an extended, perhaps solvent-swollen conformation at elevated temperatures that requires a long time to revert back to the room temperature structure. Such behavior is observed in studies of polymer gels, where varying the temperature results in the hysteresis of macroscopic polymer properties such as swelling, elasticity, turbidity, and so forth.

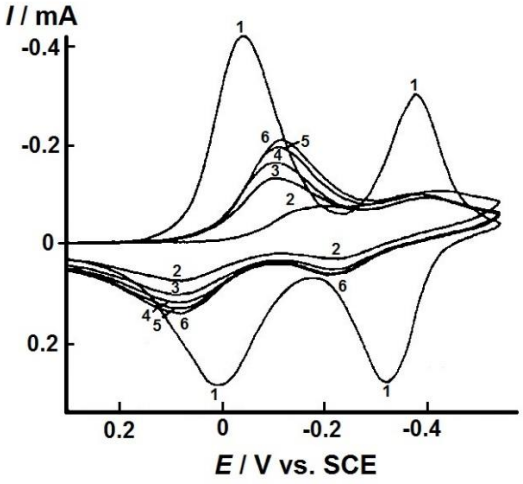

***Figure 31**. Cyclic voltammograms obtained for a poly(tetracyanoquinodimethane) electrode in contact with 10 M LiCl at (1) 69 °C and (2–6) after rapid cooling at 22 °C, recorded after delays of (2) 4, (3) 9, (4) 13.5, (5) 22.5, and (6) 38.5 min [39]*

Break-in and first cycle effects

For a range of neutral polymer films freshly deposited on metal substrates by solvent evaporation techniques several potential sweeps are required for the films to become fully electroactive. This phenomenon has been referred as the break-in effect. The break-in effect is attributed to the incorporation of solvent molecules and ions into the film phase during electrolysis, as well as to potential-dependent morphological changes. The rate of the diffusive transport of solvent molecules depends on the structure of the polymer and the motion of polymer segments. In crystalline and crosslinked polymers, or below the glass transition temperature, the movement of the incorporating species may be rather slow. On the other hand, solvent molecules act as plasticizers, and therefore increase the rate of diffusion for both neutral and ionic species inside the film.

The first cycle or waiting time effects (where the shapes of the cyclic voltammograms and the peak potentials depend on the delay time at potentials at which the polymer is in its neutral / discharged state: see also as "secondary break-in") have been interpreted in terms of slow morphological changes and / or the difficulty removing the remaining charges from insulating surroundings.

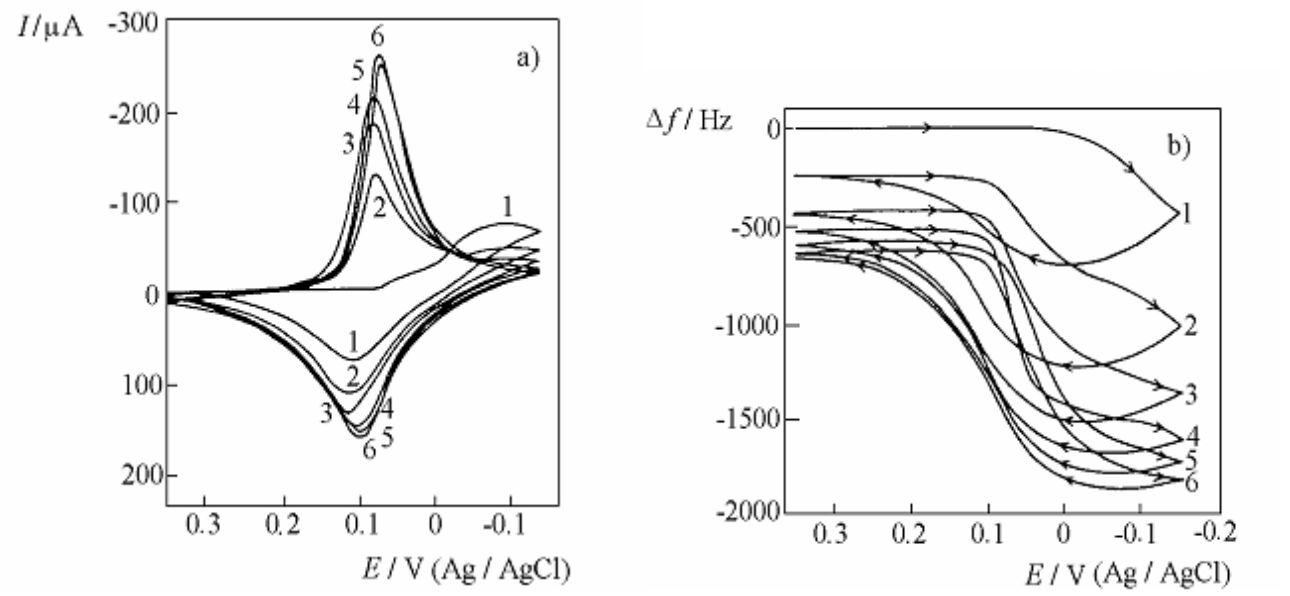

***Figure 32.** "Break-in effect," as observed in cyclic voltammetric and simultaneous EQCN measurements performed with a virgin and thick poly(tetracyanoquinodimethane) electrode. $\Gamma = 7\times10^{-8}$ mol cm^{-2}. Electrolyte: 2.5 M LiCl. Scan rate: 6 mV s^{-1}. a) Consecutive cyclic voltammograms; b) **s**imultaneously obtained EQCM frequency curves [40]*

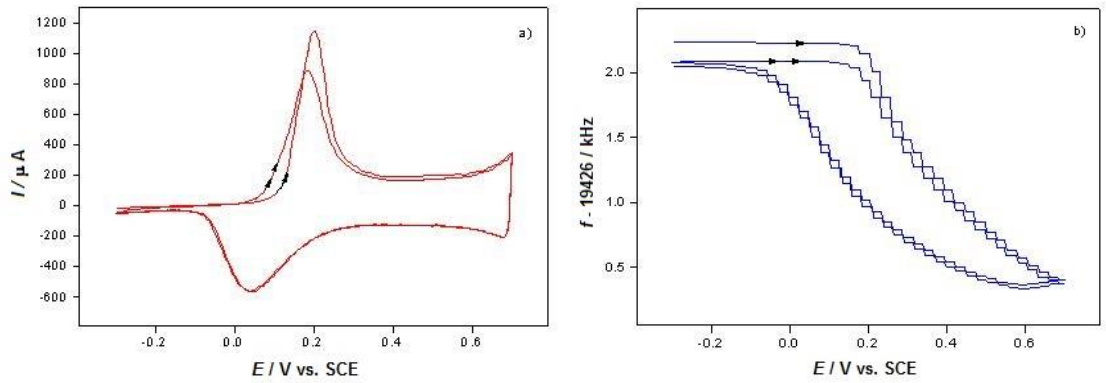

Figure 33. *Cyclic voltammograms (two cycles) a) and the simultaneously detected EQCN frequency changes b) for a polyaniline film (L = 2.9 µm) in contact with 1M H_2SO_4. Scan rate: 100 mV s^{-1} [38]*

Charging/discharging (or redox switching) processes are usually fast, but are rather complex in nature. The steady-state cyclic voltammograms in the case of polyaniline exhibit a combination of broad anodic and cathodic peaks with a plateau in the current at higher potentials (Fig. 33). The current is proportional to the scan rate, *i.e.*, from an electrical point of view the film behaves like a capacitor, however, this simple result is the consequence of a complicated phenomenon which includes a faradaic process (the generation of charged electronic entities at the polymer chains near the electrode surface by electron transfer to the metal), the transport of those species throughout the film, as well as the ion exchange at the film|solution interface. A closer inspection of the curves of Fig. 33 reveals two effects of importance. First, the so-called first-cycle effect, *i.e.*, the first anodic cycle after starting the investigation of a virgin film or after a long waiting time at negative potentials where the polymer is its reduced state, differs from the subsequent ones. The main reason is the incorporation of ions and solvent molecules, and the transformation and relaxation of the structure of the polymer layer. Second, at pH 0 in the beginning of the oxidation the mass change is minor, although a substantial amount of charge has already been injected. The low mass change is due to the low molar mass of H^+ ion, which is the species that leaves the surface layer. The incorporation of the anions, which have a much higher molar mass, clearly manifests itself in the observed EQCN frequency decrease in a later phase of oxidation at higher anodic potentials. Owing to the very high repulsion forces between the nearest-neighbor sites in the polymer chain, it is unfavorable that protons on the nitrogen atom and the benzenoid ring filled with a hole (polaron) should exist next to each other simultaneously. Consequently, deprotonation is a necessary process when positive charges are injected into the polymer.

Characterization

The complete characterization of conducting polymer and composite films, layers, membranes *etc.* includes the determination of all electrochemical properties (formal potential of the redox reaction, charge storage capacity, rates of electron transfers, rates of ionic and electronic charge transport processes, rate of solvent transport and phase equilibria, the mechanism and kinetics of the electrochemical-chemical reactions, the film morphology and all the useful properties, *e.g.*, the changes of color or conductivity. In order to achieve this goal usually several experimental techniques and their combination are needed as it had been mentioned. Furthermore, it is always worth to apply the variation of experimental conditions because in this, relatively simple way essential information can be obtained about the reaction mechanism, different interactions

between the polymer and the ions and molecules present. Two examples will be shown: the effect of the nature of electrolyte and the pH dependence.

Already the cyclic voltammograms reveal the strength of interaction between the polymer and the counter-ions but by using combined methods *e.g.*, EQCN, the transport and sorption of ions and solvent molecules can be understood by the help of such easy experiments.

Poly(vinylferrocene) is more swollen in the presence of SO_4^{2-} ions than in NO_3^- or ClO_4^-- containing electrolytes. This means that the different anions enter the film together with their hydration spheres, since the magnitude of the mass change is as follows: sulfate > nitrate > perchlorate. This corresponds to the order of degree of hydration of these anions. On the other hand, the ion-pair formation constant for the oxidized sites and the ClO_4^- - ions is greater than that for NO_3^- or SO_4^{2-} ions, which is reflected in the more positive formal potential of the ferrocene/ferricenium redox couple in Na_2SO_4 or $NaNO_3$ solutions compared with $NaClO_4$ electrolyte, as seen in Fig. 34. The more pronounced swelling also reflects the more extensive interaction between water and the charged ferricenium sites in the presence of SO_4^{2-} - or NO_3^- - compared to ClO_4^- -containing electrolytes.

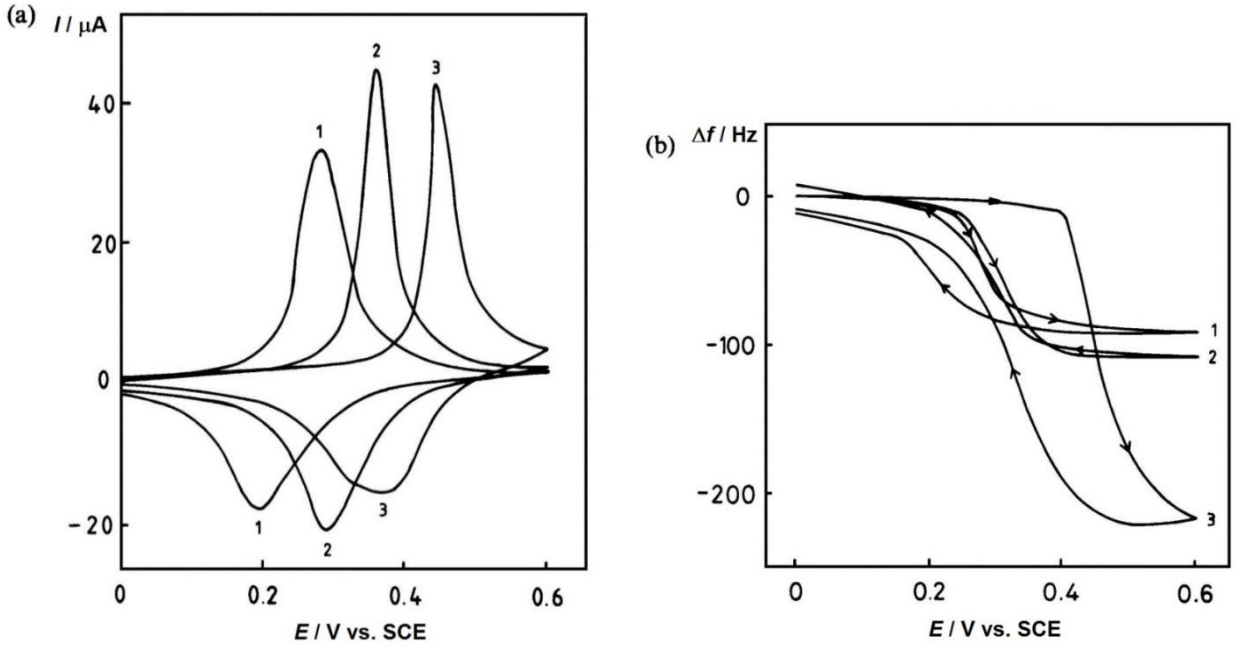

***Figure 34**. Cyclic voltammograms (**a**) and the simultaneously recorded EQCN curves (**b**) for an electrochemically deposited poly(vinylferrocene) film in contact with (1) $NaClO_4$; (2) $NaNO_3$; and (3) $Na_2SO_4|H_2SO_4$ pH 3.4, respectively. Electrolyte concentration: 0.5 mol dm^{-3}. Scan rate: 10 mV s^{-1}. [40]*

Because the polymers under study are organic compounds and/or contain groups available for protonation the execution of the experiments at different pH values is inevitable since the electron transfer steps are accompanied by protonation or deprotonation. As an example, the cyclic voltammograms obtained at different pH values in sulfate electrolytes for a poly(copper phthalocyanine) [poly(CuPc)] layer are presented (Fig. 35). It is evident that H^+ ions participate in the redox processes since with increasing pH the voltammetric peaks shift into the direction of the more negative potentials by –65 ± 5 mV/pH. Therefore, we can conclude that the redox reaction of poly(CuPc) is basically a 1 H^+/1 e^- or 2 H^+/2 e^- reaction. Albeit this reaction is much more complicated, and the electron transfers are accompanied with dimerization and morphological changes, the pH dependence serves as a starting point [41].

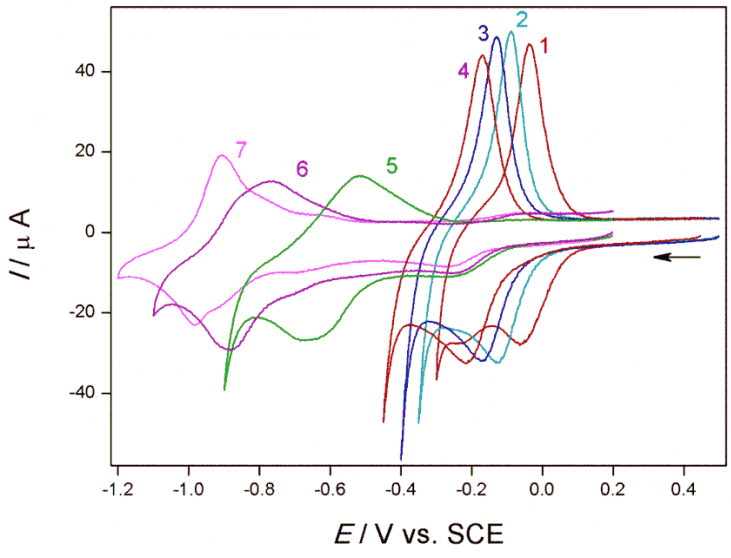

***Figure 35**. Au|poly(CuPc) electrode in contact with sulphate electrolytes (H_2SO_4 or H_2SO_4 + Na_2SO_4 or Na_2SO_4 + NaOH) pH values: 0.3 (1), 1.18 (2), 2.17 (3) 2.57, (4), 7.8 (5), 11.1 (6) and 12.7 (7). Scan rate: 10 mV s^{-1}. The total concentration of the sulfate ions was kept practically constant at 0.5 mol dm^{-3} [41]*

Applications

Material Properties of Conducting Polymers

Electronically conducting polymers can be prepared from cheap compounds such as aniline, pyrrole, thiophene and their derivatives by relatively simple chemical or electrochemical polymerization processes. Redox polymers are also applied in special cases, such as in biosensors or electrochromic display devices. Redox processes combined with the intercalation of anions or cations can therefore be used to switch the chemical, optical, electrical, magnetic, mechanic and ionic properties of such polymers. These properties can be modified by varying the anion size and preparation techniques; by including other chemical species for example. A qualitative summary of the relationship between the properties of a conducting polymer and its charge state is given in Table 1.

***Table 1.** Qualitative properties of conducting polymers that conduct in their oxidized state, as a function of their charge state [6]*

Properties/Charging state	Reduced	Oxidized
Stoichiometry	without anions (or: with cations)	with anions (or without cations)
Content of solvent	smaller	higher
Volume	smaller	higher
Color	transparent or bright	dark
Electronic conductivity	insulating, semiconducting	semiconducting, metallic
Ionic conductivity	smaller	high
Diffusion of molecules	dependent on structure	
Surface tension	hydrophobic	hydrophilic

Typical areas in which conducting polymers are applied can be described using a double logarithmic plot of ionic resistance versus electronic resistance, as shown in Fig. 36.

The positions of ideal metals, semiconductors and insulators in the diagram are shown at the top. Constant properties exist at high ionic resistances, *i.e.*, towards the top of the diagram. Here, ICPs can be applied in the dry state in an inert atmosphere. Contact with an electrolyte leads to a much wider field of applications, depending on the specific ionic and electronic resistances associated with the charge state, such as in batteries, displays, sensors, *etc.*

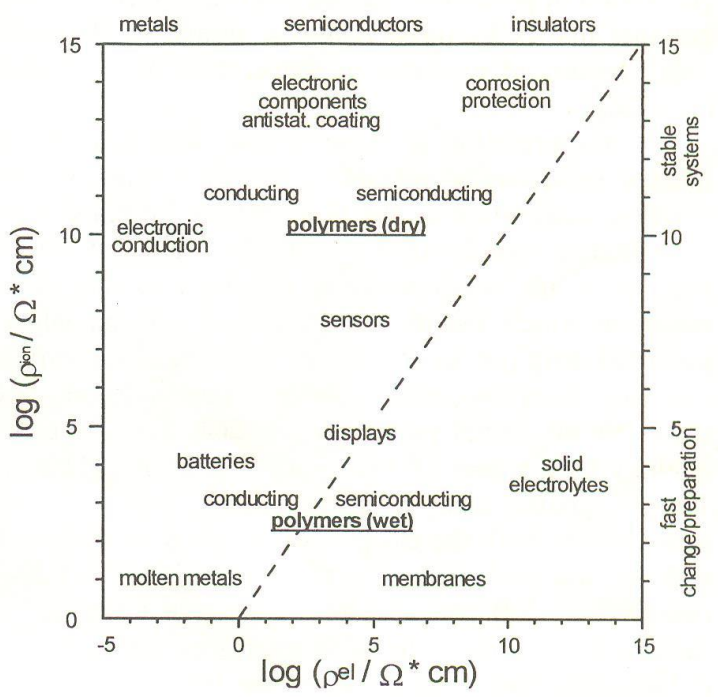

***Figure 36**. Double logarithmic plot of ionic resistance versus electronic resistance for conducting polymers, showing areas of application [6]*

Gas sensors

Gas sensors made of conducting polymers have high sensitivities and short response times, and —a great advantage compared with most commercially available sensors based on metal oxides— work at room temperature. The sensing principles employed in gas sensors using conducting polymers as active sensing materials vary. The principle used depends on the variables (resistance, current, absorbance, mass, *etc.*) measured and the type of interaction between the gas (analyte) and the polymer. The oxidation state (the charge or doping level) of the polymer is altered by the transfer of electrons from the analyte to the polymer, which causes a change in the properties (resistance, color, work function, *etc.*) of the polymer.

For instance, electron-donor gases such as NH_3 increase the resistance of polyaniline (PANI) because the electrons transferred neutralize the positive sites (polarons), and the polymer becomes neutral. Interestingly this is a reversible process; after flushing the polymer with air, the conductivity of the polymer (sensing layer) is recovered (Figs. 37-39).

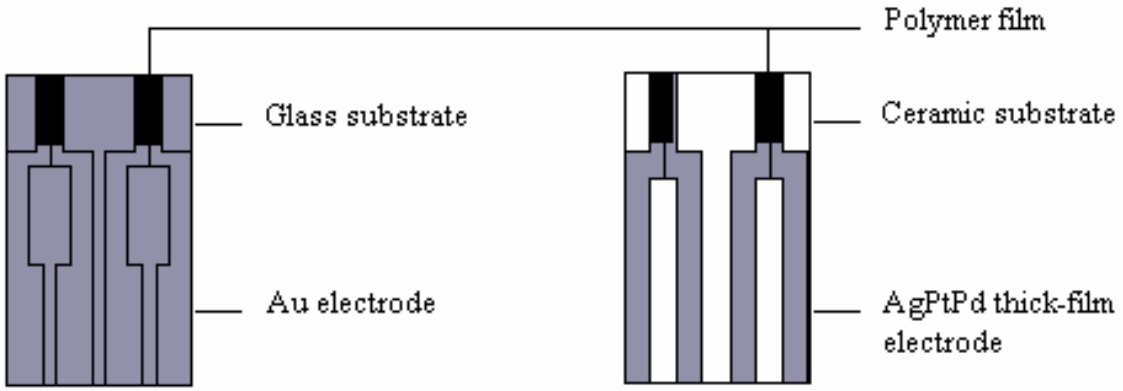

***Figure 37.** Layout designs of thin-film and thick-film polymer gas sensors [42]*

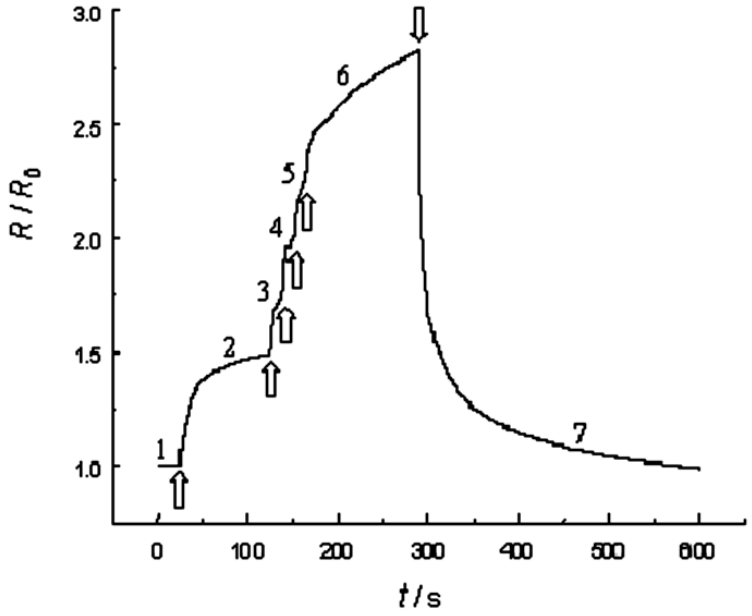

***Figure 38**. The response of a PANI gas sensor (relative resistance vs. time curves at 20 °C). 10 ppm ammonia was injected into the air at times indicated by the arrows. The total concentrations were: (1) 0, (2) 10, (3) 20, (4) 30, (5) 40, (6) 50 ppm; and (7) after flushing with clean air again [43]*

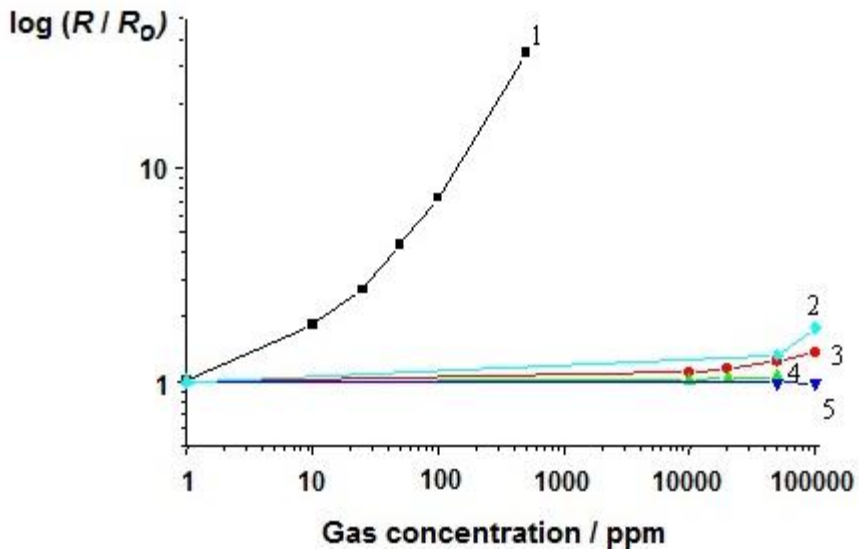

***Figure 39**. The response of a PANI ammonia sensor (log relative resistance–gas concentration plot) for different gases and vapors: (1) ammonia; (2) methanol; (3) ethanol; (4) CO; and (5) NO; at room temperature [43]*

Other sensors and biosensors

The use of conducting polymers as amperometric sensors, where the detection signal is amplified due to the catalytic properties of the polymer and / or built-in catalytic entities, is straightforward, although the application of these systems as ion-selective electrodes in potentiometry is problematic because redox state and acid–base or ionic equilibria need to be controlled simultaneously.

Poly(methylene blue) is a very good catalyst for the oxidation of hemoglobin. This property has been utilized in an amperometric sensor (see Figs. 40 and 41). A good correlation was found between the results of the electrochemical method and those of the spectrophotometric cyanidation analysis method, which is used in clinical practice as a standardized protocol [44].

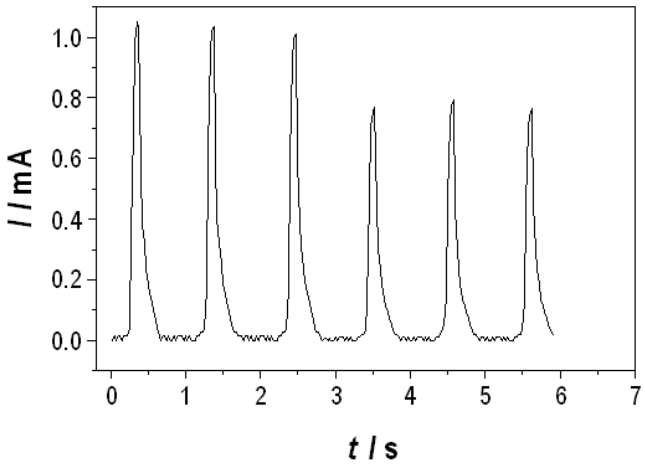

***Figure 40**. Chronoamperometric responses for consecutive injections into a flow cell of samples of whole blood diluted 1:10 in phosphate buffer (pH 6.24) and 0.5 mol dm^{-3} NaCl on a poly(methylene blue) electrode at E = 0.4 V vs. SCE. Flow rate: 4 ml min^{-1}. The tall and short waves are the responses to 6 cm^3 and 4 cm^3 dilute solutions, respectively [44]*

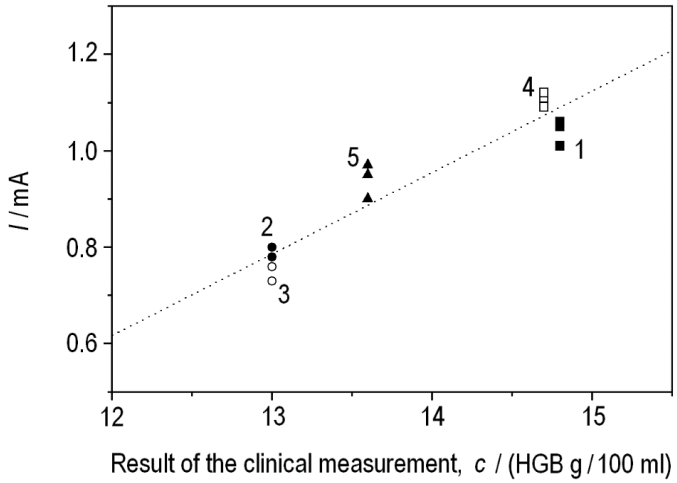

***Figure 41**. Comparison between electrochemical and cyanidation methods for the analysis of blood samples provided by five donors. Blood samples 2 and 3 were from females, while 1 and 4 were from male patients. Patients 1–4 were healthy, while patient 5 was a potentially ill donor. Experimental conditions were the same as for Fig. 40 [44]*

Electrochromic display devices

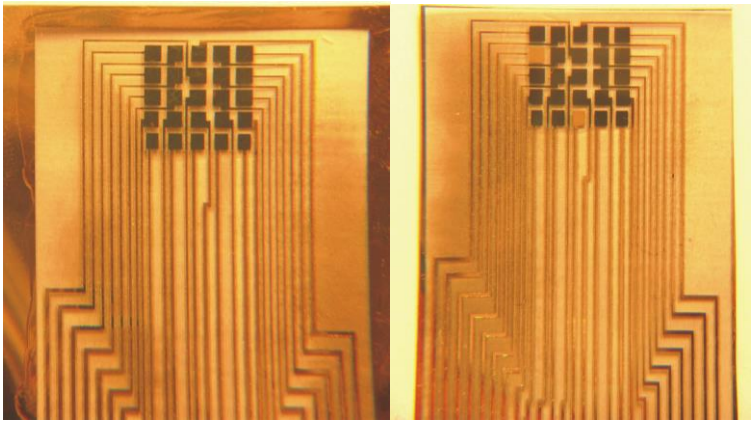

***Figure 42.** Photos of a PANI-based flexible electrochromic display device containing 25 pixels. The display region and the connections were made by depositing gold on a plastic sheet using an appropriate mask and an evaporation technique. Each pixel can be driven separately. Left: PANI is in its oxidized state in all pixels. Right: PANI is reduced in two pixels (the bleached ones)*

Due to its many advantageous properties (low cost, fast color change, good contrast, stability, *etc.*), PANI is also a favorite material for use in electrochromic display devices. Pictures of a PANI-based flexible device are shown in Fig. 42. The display pattern, which consists of 25 pixels and the connections that allow each pixel to be driven separately, was fabricated by depositing gold onto a plastic sheet. Another plastic sheet covers the display. The electrochemical switching is executed using a counter electrode, which also serves as a reference electrode, and an acidic gel electrolyte is placed between the two sealed plastic sheets.

Supercapacitors

In electric and hybrid vehicles during acceleration a high power density is needed or in backup power devices the fast response is crucial. Supercapacitors are ideal for these purposes, and that is the very reason for the intense quest regarding electrode materials, which can meet the requirements of reversibility, long-term stability, the high storage capacity and the fast charging/discharging characteristics.

Among the different metal oxides, the properly prepared hydrous RuO_2 shows the best properties. Its commercial use is, however, hindered due its high cost and limited availability. Another class of materials, which in principle is suitable for supercapacitor applications are the electrically conducting polymers. These materials are cheap, show reversible redox behavior and high capacitance, but their long-term stability is not good enough. The combinations of RuO_2 with conducting polymers seem to be a promising attempt to have a possible synergic effect, *i.e.*, simultaneously improving the electron transport, stability and decreasing the cost. A simple method resulting in a well-defined, well-dispersed RuO_2–polyaniline composite on the electrode surface is the use of the oxidation power of Ru (IV) that is the ability of RuO_2 crystals attached to the electrode surface to oxidize the aniline which process resulting in the formation of PANI on the external and internal surfaces of RuO_2 crystals [45]. The EQCN frequency decrease indicates the deposition of polyaniline (Fig. 42). The reduced ruthenium sites can be regenerated by using short positive potential pulses (Fig. 43).

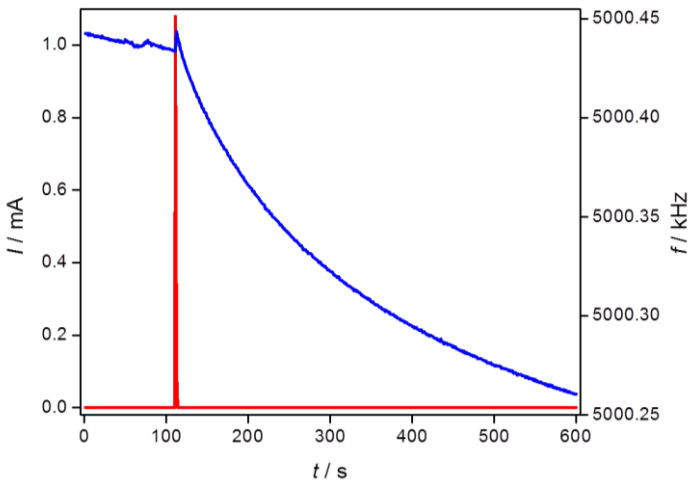

Figure 42. *(a) The EQCN frequency change vs. time curve (blue) observed for an Au|RuO_2 electrode after the addition of aniline into 0.5 M H_2SO_4 solution at open-circuit potential (0.85 V). The RuO_2 has been oxidized previously (current peak) [45]*

The respective cyclic voltammograms and EQCN curves are displayed in Figs. 44-46. After the first deposition step the response of the polyaniline appears, however, the response originating from RuO_2 dominates. Following further deposition steps the mass change during cycling also becomes higher, however, in the potential region of the leucoemeraldine – emeraldine transition, *i.e.*, from

–0.1 to 0.15 V the frequency change is mostly due to processes occurring simultaneously with the oxidation of the lower valence Ru sites. In acid media the EQCN response of the PANI is minor because only deprotonation takes place, and H^+ ions leave the surface phase. On the other hand, after the peak the incorporation of anions manifests itself in a frequency decrease. The effect of PANI is even better seen when a more positive switching potential is applied. At more positive potentials the second pair of waves due to the transition of the emeraldine form to pernigraniline form is nicely seen. In this case the redox transformation is accompanied by the desorption of anions and H^+ ions which causes a substantial mass loss.

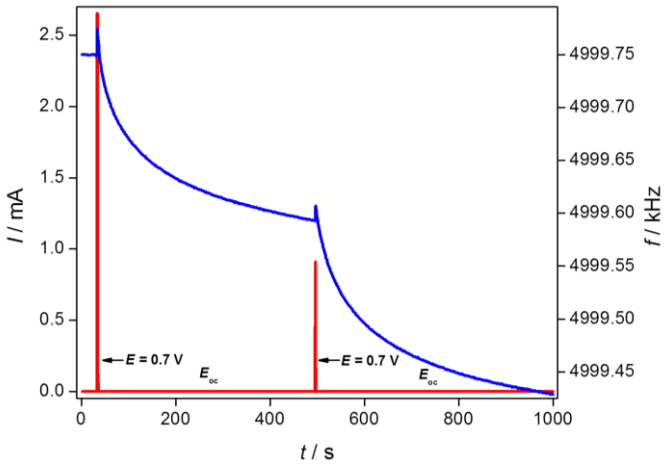

Figure 43. *The continuation of the experiment presented in Fig. 42. The EQCN frequency change* vs. *time curve observed for the Au | RuO_2 electrode after two additional reoxidation pulses [45]*

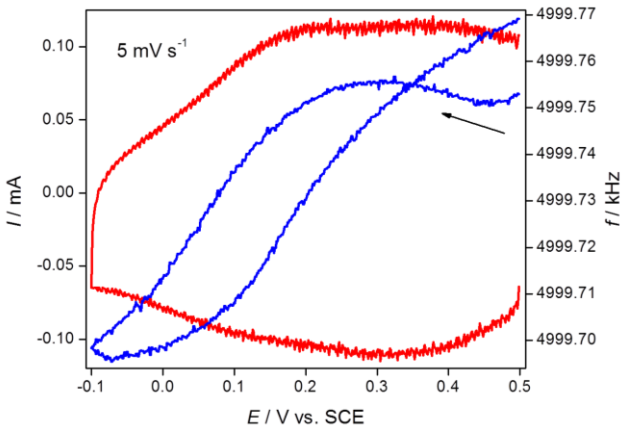

Figure 44. *Cyclic voltammogram (red) and the simultaneously obtained EQCN frequency response (blue) for the Au | RuO_2 + PANI electrode prepared above. Scan rate: 5 mV s^{-1}, Potential range: –0.15 – 0.5 V. Electrolyte: 0.5 M H_2SO_4 [45]*

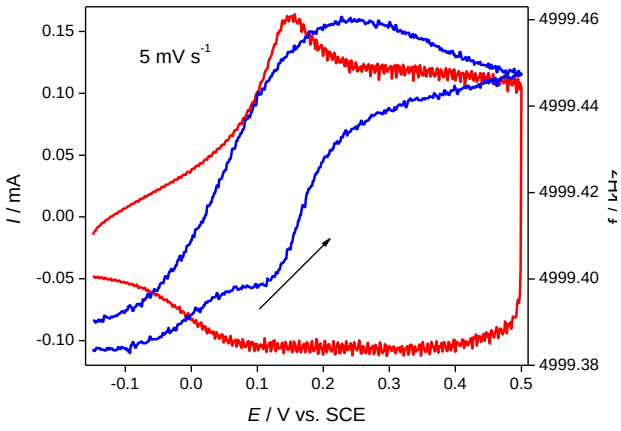

Figure 45. *Cyclic voltammogram (red) and the simultaneously obtained EQCN frequency response (blue) for the Au | RuO_2 + PANI electrode after three successive activation pulses. Scan rate: 5 mV s^{-1}, Potential range: –0.15 – 0.5 V. Electrolyte: 0.5 M H_2SO_4 [45]*

Fig. 46 shows the cyclic EQCN responses by using an extended potential range at pH 3.5.

One of the important features of the RuO_2/PANI composite is that the electrochemical activity of the polyaniline is remarkably preserved at higher pH values even at pH 7 a reasonable capacitive response can be obtained. For the RuO_2 samples used in this study in contact with 0.5 M H_2SO_4 solution the specific capacitance was found to be 540 $\pm$ 40 F g^{-1} in the potential range of –0.1 and 0.85 V at a scan rate of 20 mV s^{-1}. By PANI deposition, the specific capacitance can be increased as high as by 50 % without practical deterioration of the response time or stability. After successive

cycling in sulfuric acid the capacitance loss is not higher than 10-15 % after 1000 cycles. Even in some cases there is an increase of capacitance during cycling which is most likely due to the completion of hydration and sorption of electrolyte which enhances the ionic charge transfer in the pores of RuO_2 and polyaniline.

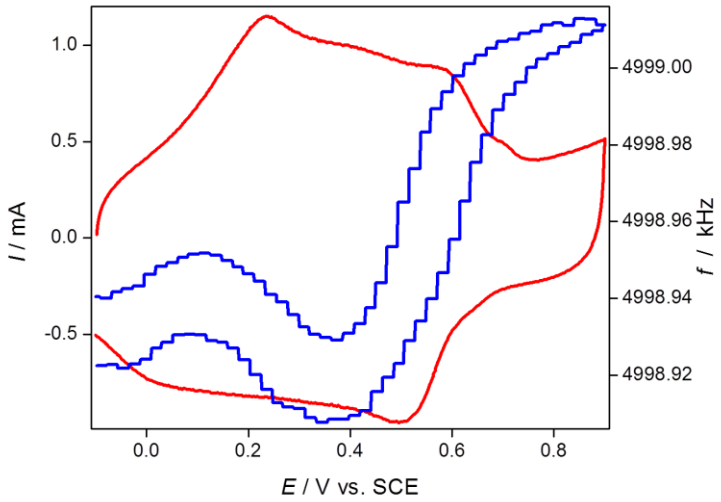

Figure 46. *Cyclic voltammogram (red) and the simultaneously obtained EQCN frequency response (blue) for the Au│ RuO_2 + PANI electrode after three successive activation pulses. Scan rate: 50 mV s^{-1}, Potential range: - 0.15 – 0.9 V. Electrolyte: 0.5 M H_2SO_4 + Na_2SO_4 pH 3.5 [45]*

New trends

In the last two decades the researchers have started to apply novel approaches. The new trend is the fabrication of composites including nanocomposites of polymers and other materials such as carbon nanotubes, graphene or inorganic compounds having special structure and properties. In sensors and biosensors of different kinds (conductometric, impedimetric, potentiometric, amperometric and voltammetric) conducting polymers are used as active, sensing or catalytic layers, however, in the majority of applications those serve as matrices entrapping enzymes or other biologically active compounds. The biocompatibility of several conducting polymers provides opportunity for the application in medicine as artificial muscles and limbs, as well as artificial nerves. The biomimetic (bionic) applications certainly will continue in the future. Microsystem technologies have been replacing by nanosystem technologies. More sophisticated and combined techniques have been developed, and have become widespread tools in the laboratories all around the world; *e.g.*, scanning microscopies, or the new versions of electrochemical quartz crystal nanobalance.

In the recent years we have reached a deeper level of understanding of the behavior of these systems that we can use to improve the performance of the devices based or use conducting polymers. The improvement occurs either by a fine-tuning of already promising systems or by using more sophisticated compositions and structures. Less often a quest of entirely novel applications has also been reported, however, most of the directions have already been set out 10-30 years ago. The use of the derivatives of the monomers or copolymerization of different monomers may be an option to obtain conducting polymers, which are more flexible or rigid or even crystalline for *e.g.*, heterojunction solar cells, as well as which are mechanically and chemically more stable, have a more advantageous processability *etc.* The functionalization of conducting polymers, which leads to smart materials interacting and responding to their environment, is also a great opportunity. The preparation of self-doped polymers is also a good way to overcome the problems of the ionic charge

transport during redox switching and other limitations of the use of the polymer. The other possibility is a combination of the arsenal of materials science with chemistry (electrochemistry) to improve the properties for special purposes. Nanocomposites, hybrid materials based on conducting polymers certainly become and will be important materials in the future. There is a high expectation concerning electroconducting nanomaterials such as nanofibers, nanorods and other nanostructures based on the supramolecular self-assembly of conducting polymers, *e.g.*, in the enhancement of the photoluminescence efficiency by utilization of the energy and charge transfer effect in surface resonance coupling. Manipulation of the microstructures of polymers may improve the performances of both the polymer-based transistors and electrochemical cells. There will be tasks for the chemists, electrochemists in the production and characterization of new materials, for the theoreticians to explain the phenomena observed or will be observed and to predict new opportunities, and also engineers to give a final form of the devices. The conducting polymers are relatively cheap materials; however, the specially improved properties can give a further boost concerning the mass production, which makes the products much less expensive. For instance, making ink from conducting polymers opens up new horizons for printing sensors, electronic circuits, solar cells, light emitting displays *etc.* The new trends can nicely be followed by studying the literature including papers and the topics of conferences.

Conclusions

Based on the review of the achievements during the last 40 years we can draw the conclusion that the development in the field of conducting polymers is unbroken, and we still expect new discoveries and novel utilizations in several areas such as energy storage and power sources, photovoltaics, health care, and different technologies.

References

[1] G. Inzelt, Recent advances in the field of conducting polymers. *Journal of Solid State Electrochemistry* **21** (2017) 1965–1975.
[2] G. Inzelt, *Conducting polymers - A new era in electrochemistry,* 2nd edn. In: F. Scholz (ed) Monographs in electrochemistry, Springer, Heidelberg, Berlin, Germany, 2012.
[3] G. Inzelt, Journal of Solid State Electrochemistry **15** (2011) 1711-1718.
[4] G. Inzelt: *Mechanism of Charge Transport in Polymer Modified Electrodes*, In: Electroanalytical Chemistry, A Series of Advances, A.J. Bard (ed.), Vol. 18, Marcel Dekker, Inc., New York, USA, 1994. pp. 89-241.
[5] G. Inzelt, *Charge transport in polymer modified electrodes*, Encyclopedia of Electrochemistry, A.J. Bard, M. Stratmann (eds.) Functions and applications of modified electrodes Vol. 10, I. Rubinstein, J. Rusling, M. Fujihara (eds.), Weinheim, Wiley-VCH, 2007. Ch. 9, pp. 651-683.
[6] G. Inzelt, M. Pineri, J.W. Schultze, M.A. Vorotyntsev, *Electrochimica Acta* **45** (2000): 2403-2421.
[7] E. Csahók, E. Vieil, G. Inzelt, *Journal of Electroanalytical Che*mistry **482** (2000) 168-177.
[8] G. Inzelt, E. Csahok,V. Kertész, *Electrochimica Acta* **46** (2001) 3955-3962.
[9] H. Shirakawa, E. J. Louis, A. G. MacDiarmid, C. K. Chiang, A. J. Heeger, *Journal of Chemical Society Chemical Commununications* (1977) 579-580.
[10] C. K. Chiang, C. R, Fischer, Y.W. Park, A. J. Heeger, H. Shirakawa, E. J. Louis S. C. Gau, A. G. MacDiarmid, *Physical Review Letters* **39** (1977) 1098-1101.
[11] C. K. Chiang, M. A. Druy, S. C. Gau, A. J. Heeger, E. J. Louis, A. G. MacDiarmid, Y. W.Park, H. Shirakawa, *Journal of American Chemical Society* **100** (1978) 1013-1015.
[12] H. Shirakawa Angewandte Chemie International Edition **40** (2001) 2574-2580.
[13] A. G. MacDiarmid, *Angewandte Chemie International Edition* **40** (2001) 2581-2590.
[14] A. J. Heeger, *Angewandte Chemie International Edition* **40** (2001) 2591-2611.
[15] H. Letheby *Journal of Chemical Society* **15** (1862) 161-163.

[16] J. Fritzsche, Journal für praktische Chemie, 20 (1840) 453–457.
[17] N. E. Khomutov, S. V. Gorbachev *Zhurnal Fizichekoi Khimii* **24** (1950) 1101-1106.
[18] D. M. Mohilner, R. N. Adams, W. J. Argersinger, *Journal of Electrochemical Society* **84** (1962) 3618-3622.
[19] R. deSurville, M. Josefowicz, L. T. Yu, J. Perichon, R. Buvet, *Electrochimica Acta* **13** (1968) 1451-1458.
[20] A. F. Diaz, J. A. Logan, *Journal of Electroanalytical Che*mistry **111** (1980) 111-114.
[21] G. Inzelt, G.G. Láng: *Electrochemical Impedance Spectroscopy (EIS) for Polymer Characterization* In: Electropolymerization (eds. S. Cosnier and A. Karyakin) Wiley-VCH, Weinheim, Germany, 2010, pp. 51-76.
[22] Electroanalytical Methods, Guide to Experiments and Applications 2nd, revised and extended edition (ed. F. Scholz), Springer-Verlag, Berlin Heidelberg, 2010.
[23] Cs. Visy, In situ combined electrochemical techniques for conducting polymers, Springer, Berlin, Heidelberg, 2017.
[24] G. G. Láng, C. A. Barbero, *Laser techniques for the study of electrode.* In: F. Scholz (ed) *Monographs in electrochemistry*. Springer, Berlin, Heidelberg, 2012.
[25] J. Heinze, B. A. Frontana-Uribe, S. Ludwigs, *Chemical Reviews* **110** (2010) 4724-4771
[26] Electropolymerization (eds. S. Cosnier and A. Karyakin) Wiley-VCH, Weinheim, Germany, 2010.
[27] B. B. Berkes, Á. Nemes, C. E. Moore, F. Szabó, G. Inzelt, *Journal of Solid State Electrochemistry* **17** (2013) 3067–3074.
[28] S. Pruneanu, E. Csahók, V. Kertész, G. Inzelt, *Electrochimica Acta* **43** (1998) 2305-2323.
[29] B. B. Berkes, G. Inzelt, E. Vass, *Electrochimica Acta* **96** (2013) 51-60.
[30] B. B. Berkes, G. Inzelt, *Electrochimica Act*a **122** (2014) 11-15.
[31] B. B. Berkes, A. S. Bandarenka, G. Inzelt, *Journal of Physical Chemistry C – Nanomaterials and Interfaces* **119** (2015) 1996-2003.
[32] G. Inzelt, R.W. Day, J.F. Kinstle, J.Q. Chambers, *Journal of Physical Chemistry* 87 (1983) 4592-4598.
[33] G. Inzelt, G. Horányi, *Journal of Electroanalytical Chemistry*, **230** (1987) 257-265.
[34] B. B. Berkes, S. Vesztergom, G. Inzelt, *Journal of Electroanalytical Che*mistry **719** (2014) 41–46.
[35] G. Inzelt, L. Szabó, J. Q. Chambers, R. W. Day, *Journal of Electroanalytical Chemistry*, **242** (1988) 265-275.
[36] G. Inzelt, Journal of Electroanalytical Chemistry, **279** (1990) 169-178.
[37] G. Inzelt, J. Q. Chambers, J. Bácskai, R. W. Day, *Journal of Electroanalytical Chemistry*, **201** (1986) 301-314.
[38] G. Inzelt, *Electrochimica Acta* **45** (2000) 3865-3876.
[39] J. Bácskai, G. Inzelt, *Journal of Electroanalytical Chemistry* **310** (1991) 379-389
[40] G. Inzelt, J. Bácskai, *Electrochimica Acta* **37** (1992) 647-654.
[41] K. Borsos, G. Inzelt, *Journal of Solid State Electrochemistry* **19** (2015) 2565–2577.
[42] G. Harsányi, M. Réczey, R. Dobay, I. Lepsényi, Zs. Illyefalvi – Vitéz, J. Van den Steen, A. Vervaet, W. Reinert, J. Urbancik, A. Guljajev, Cs. Visy, Gy. Inzelt, I. Bársony, *Sensor Review*, **19** (1999) 128 – 134.
[43] I. Lepcsényi, A. Reichardt, G. Inzelt, G. Harsányi, *Proceeding of 12th European Microelectronics and Packaging Conference*, Harrogate, UK, 1999. pp. 301-305.
[44] C. M. A. Brett, G. Inzelt, V. Kertesz, *Analytica Chimica Acta*, **385** (1999) 119-123.
[45] S. Sopcic, M. Kraljic-Rokovic, Z. Mandic, G. Inzelt, *Journal of Solid State Electrochemistry*, **14** (2010) 2021-2026.